

Chapter 5

Quantifying Human-Image Imitation Activities

5.1 Introduction

In this chapter, we present the results of the experiments of human-image imitation activities (Section 4.5.1) which include time series, minimum embedding parameters, RSS with UTDE, RPs, RQAs and the weaknesses and strengthens of RQA.

5.2 Time series

For an easy comparison, we consider time series for only three participants (*p04, p05, p10*) with a window length of 500 samples (10-sec). Hence, Figs 5.1 and 5.3 show the time series for arm movements of participants following an image while not hearing a beat and Figs 5.2 and 5.4 show the time series for arm movements of participants following an image while hearing a beat. The remained time series are presented in Appendix D. Similarly, three levels of smoothness of normalised time series are applied to each of the cases of the experiment based on two different Savitzky-Golay filter lengths (29 and

Quantifying Human-Image Imitation Activities

159) with the same polynomial degree of 5 using `sgolay(p,n,m)` (signal R developers, 2014).

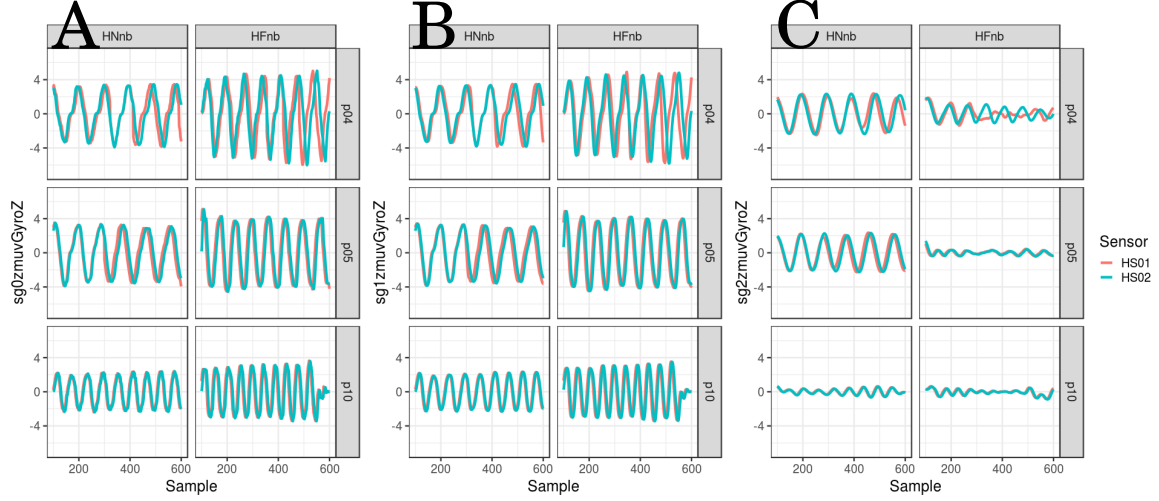


Fig. 5.1 Time series for horizontal arm movements (no beat). (A) raw-normalised (`sg0zmuvGyroZ`), (B) normalised-smoothed 1 (`sg1zmuvGyroZ`) and (C) normalised-smoothed 2 (`sg2zmuvGyroZ`). Time series are for only three participants (p04, p05, and p10) for horizontal movements in normal and faster velocity with no beat (HNnb, HFnb) using the normalised GyroZ axis (`zmuvGyroZ`) and two sensors attached to the participant wrist (HS01, HS02). R code to reproduce the figure is available from Xochicale (2018).

5.3 Minimum Embedding Parameters

5.3.1 Minimum dimension embedding values

Values of minimum embedding dimensions for horizontal normal arm movements with no beat (HNnb) and horizontal faster arm movements with no beat (HFnb) are shown in Fig 5.5 which values of minimum embedding dimensions present a fluctuation of values between four and seven over six participants. It can also be noted a slightly variation of minimum embedding dimension values over participants when comparing HS01 and HS02 (Fig 5.5(A, B)). With regards to the smoothness of the time series,

5.3 Minimum Embedding Parameters

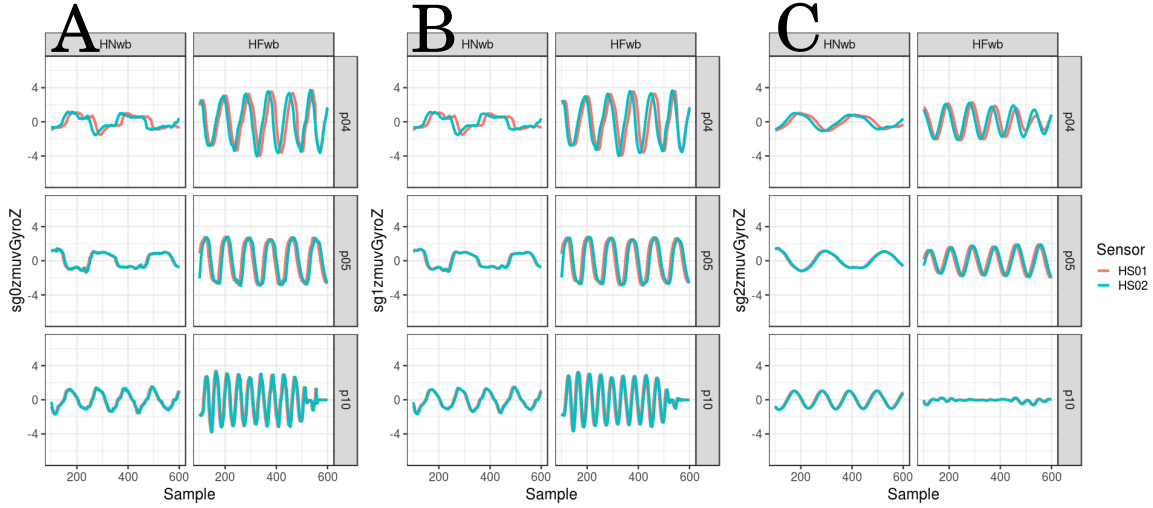


Fig. 5.2 Time series for horizontal arm movements (with beat). (A) raw-normalised ($sg0zmuvGyroZ$), (B) normalised-smoothed 1 ($sg1zmuvGyroZ$) and (C) normalised-smoothed 2 ($sg2zmuvGyroZ$). Time series are for only three participants (p04, p05, and p10) for horizontal movements in normal and faster velocity with beat (HNwb, HFwb) using the normalised GyroZ axis ($zmuvGyroZ$) and two sensors attached to the participant wrist (HS01, HS02). R code to reproduce the figure is available from Xochicale (2018).

the minimum embedding values are also smoothed showing less variations of values over six participants (Fig 5.5).

Values of minimum embedding dimension for horizontal normal arm movements with beat (HNwb) and horizontal faster arm movements with beat (HFwb) are shown in Fig 5.6 where is shown a fluctuations of values for minimum embedding dimension between five and seven. Similarly as in Fig 5.5, Fig 5.6 show changes of minimum embedding dimension between participants and the smoothness of the time series also affects the smoothness of minimum embedding dimension values.

Values of minimum embedding dimension for vertical arm movements with no beat are shown in Figs 5.7(A, B) where the smoothness of the time series have little effect on the minimum embedding dimension values, whereas smoothness of time series affects the smoothness of the minimum embedding values for vertical faster arm movements with no beats (Fig 5.7(C, D)).

Quantifying Human-Image Imitation Activities

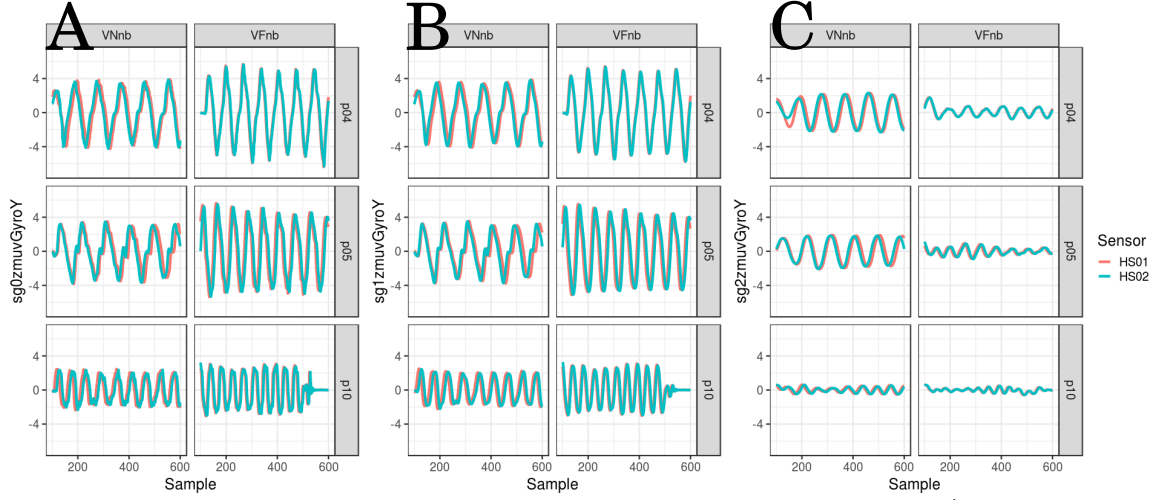


Fig. 5.3 Time series for vertical arm movements (no beat). (A) raw-normalised ($sg0zmuvGyroY$), (B) normalised-smoothed 1 ($sg1zmuvGyroY$) and (C) normalised-smoothed 2 ($sg2zmuvGyroY$). Time series are for only three participants (p04, p05, and p10) for vertical movements in normal and faster velocity with no beat (VNnb, VFnb) using the normalised GyroY axis ($zmuvGyroY$) and two sensors attached to the participant wrist (HS01, HS02). R code to reproduce the figure is available from Xochicale (2018).

Fig 5.8 shows the variation of minimum embedding values for vertical arm movements with beat where the smoothness of the time series affects both vertical normal and vertical faster movements with a slight decrease on each of the values as the smoothness increase.

5.3.2 Minimum delay embedding values

The general behavior for horizontal and vertical arm movements with regards to the smoothness of the time series is that the first minimum AMI values increase as the increase of the smoothness which is due to smoothed AMI curves (Figs 5.9, 5.10, 5.11 and 5.12).

Fluctuations of minimum AMI values from sensor HS01 are more evident than for sensor HS02 for horizontal normal arm movements with no beat (Fig 5.9(A, B)), whereas fluctuations of minimum AMI values from sensors HS01 and HS02 for horizontal

5.3 Minimum Embedding Parameters

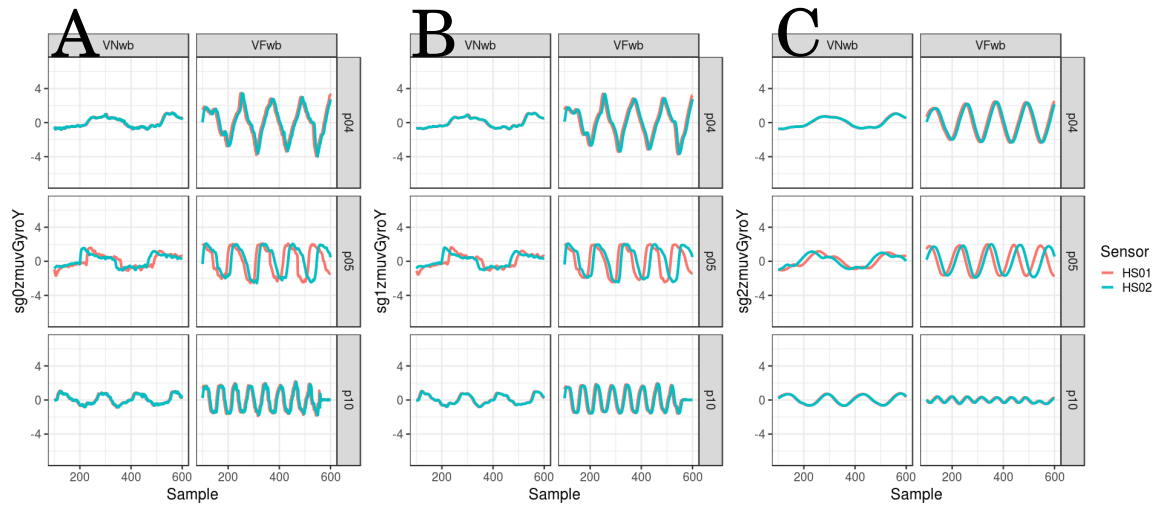


Fig. 5.4 Time series for vertical arm movements (with beat). (A) raw-normalised ($sg0zmuvGyroY$), (B) normalised-smoothed 1 ($sg1zmuvGyroY$) and (C) normalised-smoothed 2 ($sg2zmuvGyroY$). Time series are for only three participants (p04, p05, and p10) for vertical movements in normal and faster velocity with beat (VNwb, VFwb) using the normalised GyroY axis ($zmuvGyroY$) and two sensors attached to the participant wrist (HS01, HS02). R code to reproduce the figure is available from Xochicale (2018).

faster arm movements with no beat appear to be similar (Fig 5.9(C, D)). Similarly, fluctuations of minimum AMI values are more evidently for horizontal normal arm movements with beat (Fig 5.10(A, B)) than horizontal faster arm movements with beat (Fig 5.10(C, D)).

As smoothness increase, minimum AMI values for vertical normal arm movements with no beat appear to fluctuate more (Figs 5.11(A, B)) than vertical faster arm movements with no beat (Figs 5.11(C, D)), whereas for vertical normal and vertical faster arm movements with beat the fluctuation of minimum AMI values is more evidently, specially when comparing vertical normal arm movements (Figs 5.12(A, B)) with vertical faster arm movements (Figs 5.12(C, D)).

Quantifying Human-Image Imitation Activities

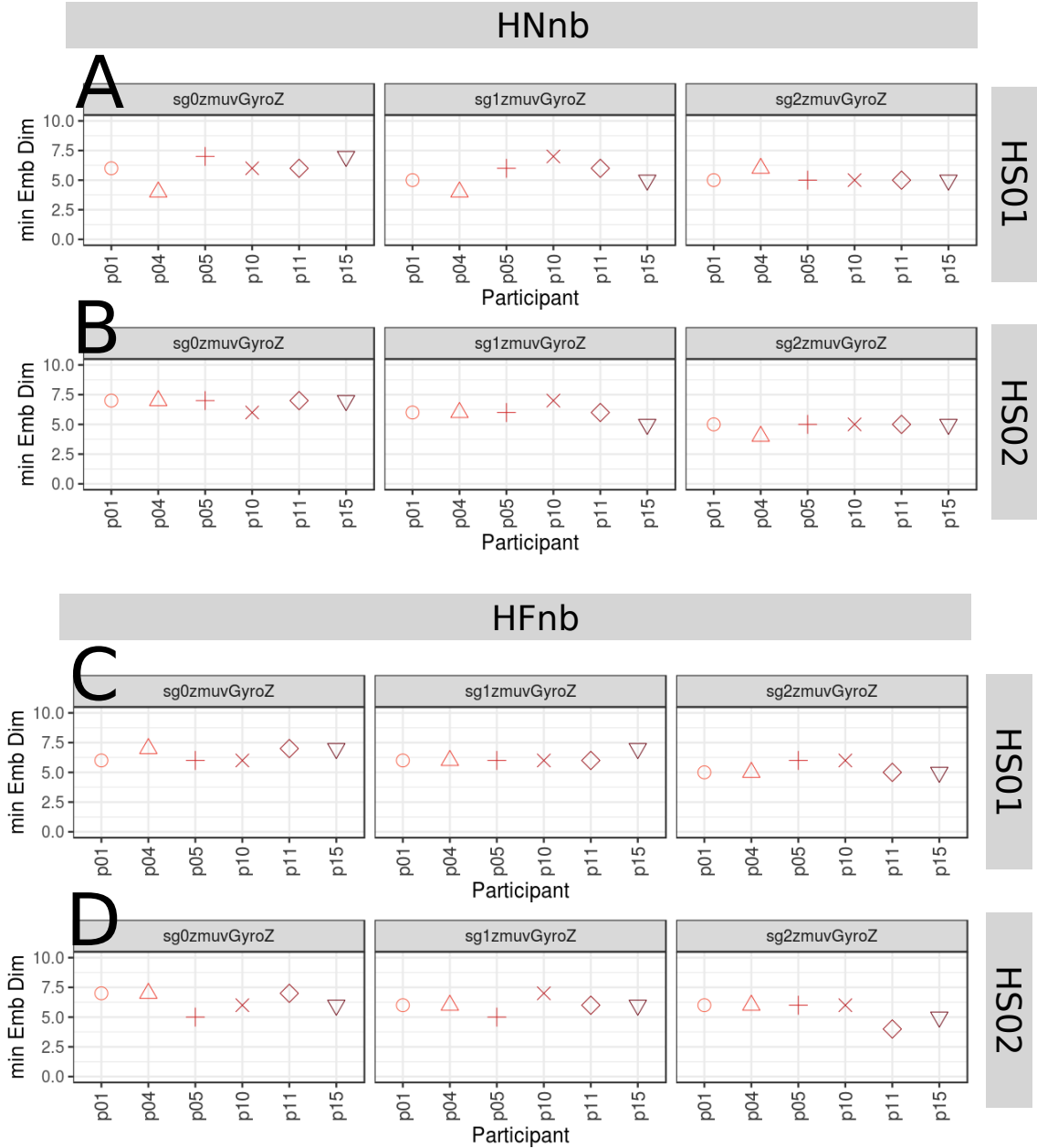


Fig. 5.5 **Minimum embedding dimensions for horizontal arm movements (no beat).** (A, B) Horizontal Normal with no beat (HNnb), and (C, D) Horizontal Faster with no beat (HFnb) movements. (A, C) Sensor 01 attached to the participant (HS01), and (B, D) sensor 02 attached to the participant (HS02). Minimum embedding dimensions are for six participants (p01, p04, p05, p10, p11, p15) with three smoothed signals (sg0zmuvGyroZ, sg1zmuvGyroZ and sg2zmuvGyroZ) and window lenght of 10-sec (500 samples). R code to reproduce the figure is available from Xochicale (2018).

5.3 Minimum Embedding Parameters

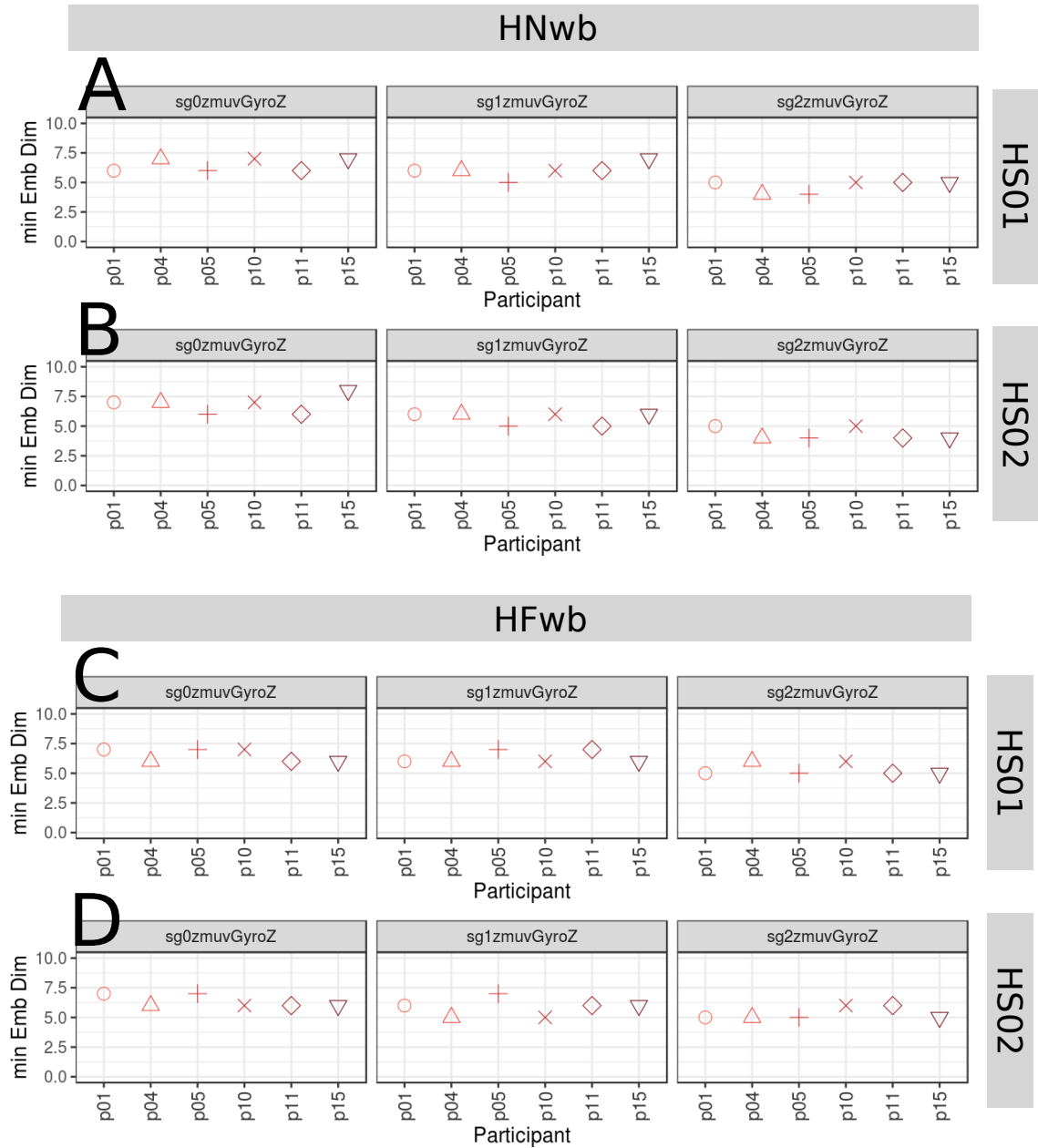


Fig. 5.6 Minimum embedding dimensions for horizontal arm movements (with beat). (A, B) Horizontal Normal with beat (HNwb), and (C, D) Horizontal Faster with beat (HFwb) movements. (A, C) Sensor 01 attached to the participant (HS01), and (B, D) sensor 02 attached to the participant (HS02). Minimum embedding dimensions are for six participants (p01, p04, p05, p10, p11, p15) with three smoothed signals (sg0zmuvGyroZ, sg1zmuvGyroZ and sg2zmuvGyroZ) and window lenght of 10-sec (500 samples). R code to reproduce the figure is available from Xochicale (2018).

Quantifying Human-Image Imitation Activities

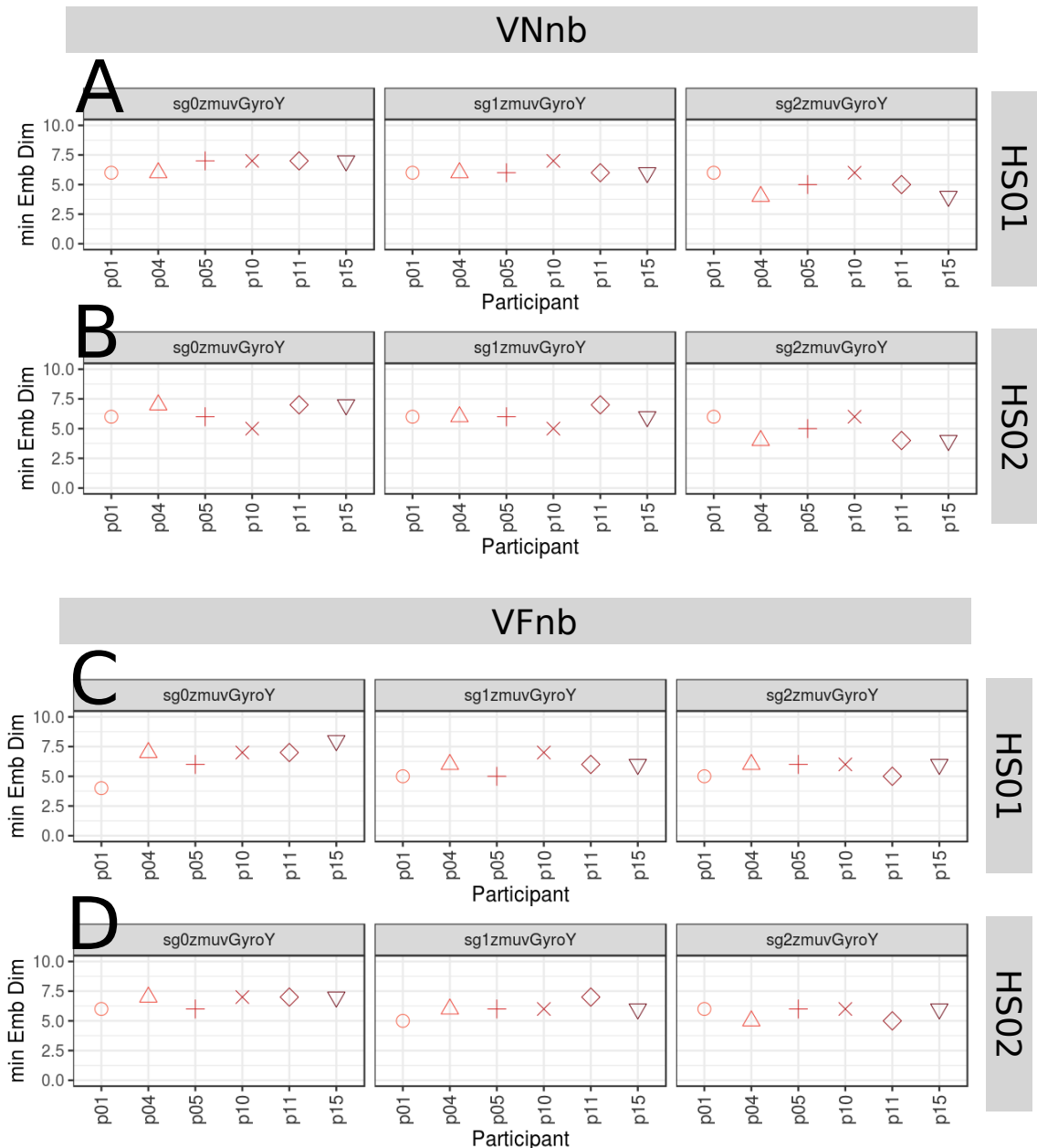


Fig. 5.7 **Minimum embedding dimensions for vertical arm movements (no beat).** (A, B) Vertical Normal with no beat (VNb), and (C, D) Vertical Faster with no beat (VFnb) movements. (A, C) Sensor 01 attached to the participant (HS01), and (B, D) sensor 02 attached to the participant (HS02). Minimum embedding dimensions are for six participants (p01, p04, p05, p10, p11, p15) with three smoothed signals (sg0zmuvGyroZ, sg1zmuvGyroZ and sg2zmuvGyroZ) and window lenght of 10-sec (500 samples). R code to reproduce the figure is available from Xochicale (2018).

5.3 Minimum Embedding Parameters

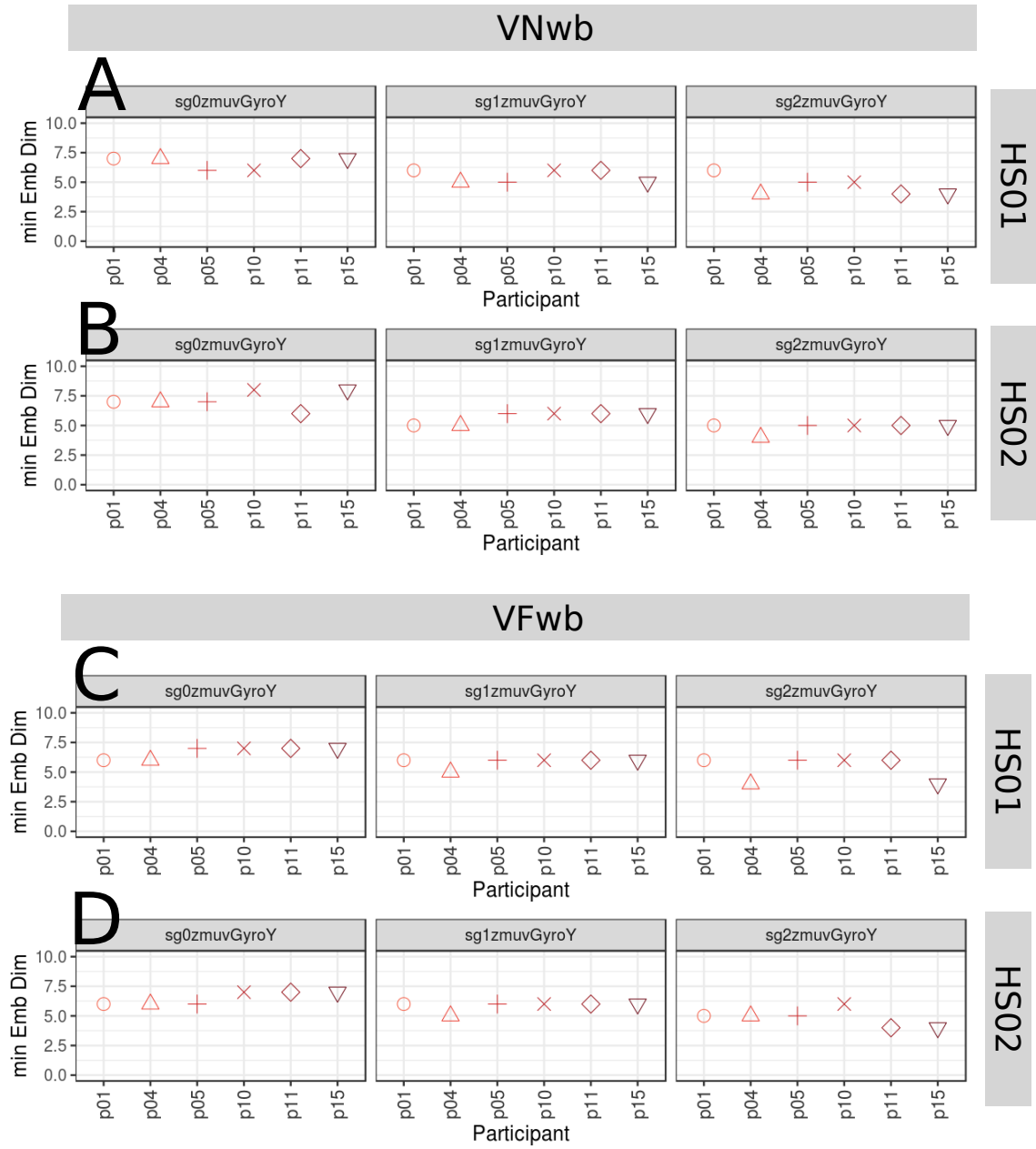


Fig. 5.8 Minimum embedding dimensions for vertical arm movements (with beat). (A, B) Vertical Normal with beat (VNwb), and (C, D) Vertical Faster with beat (VFwb) movements. (A, C) Sensor 01 attached to the participant (HS01), and (B, D) sensor 02 attached to the participant (HS02). Minimum embedding dimensions are for six participants (p01, p04, p05, p10, p11, p15) with three smoothed signals (sg0zmuvGyroZ, sg1zmuvGyroZ and sg2zmuvGyroZ) and window lenght of 10-sec (500 samples). R code to reproduce the figure is available from Xochicale (2018).

Quantifying Human-Image Imitation Activities

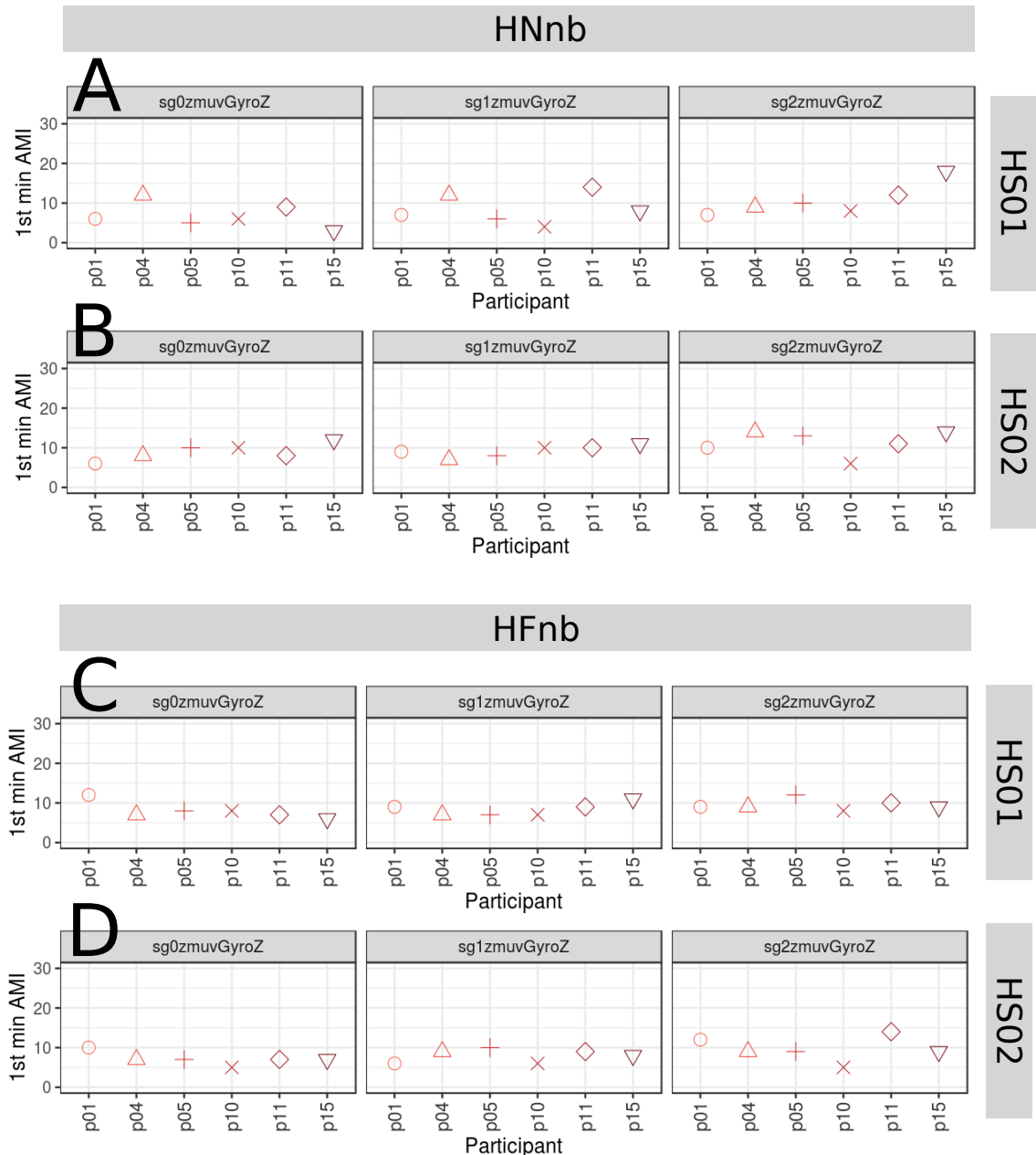


Fig. 5.9 **First minimum AMI values for horizontal arm movements (no beat).** (A, B) Horizontal Normal with no beat (HNnb), and (C, D) Horizontal Faster with no beat (HFnb) movements. (A, C) Sensor attached to the participant (HS01), and (B, D) sensor attached to the participant (HS02). First minimum AMI values are for six participants (p01, p04, p05, p10, p11, p15) with three smoothed signals (sg0zmuvGyroZ, sg1zmuvGyroZ and sg2zmuvGyroZ) and window lenght of 10-sec (500 samples). R code to reproduce the figure is available from Xochicale (2018).

5.3 Minimum Embedding Parameters

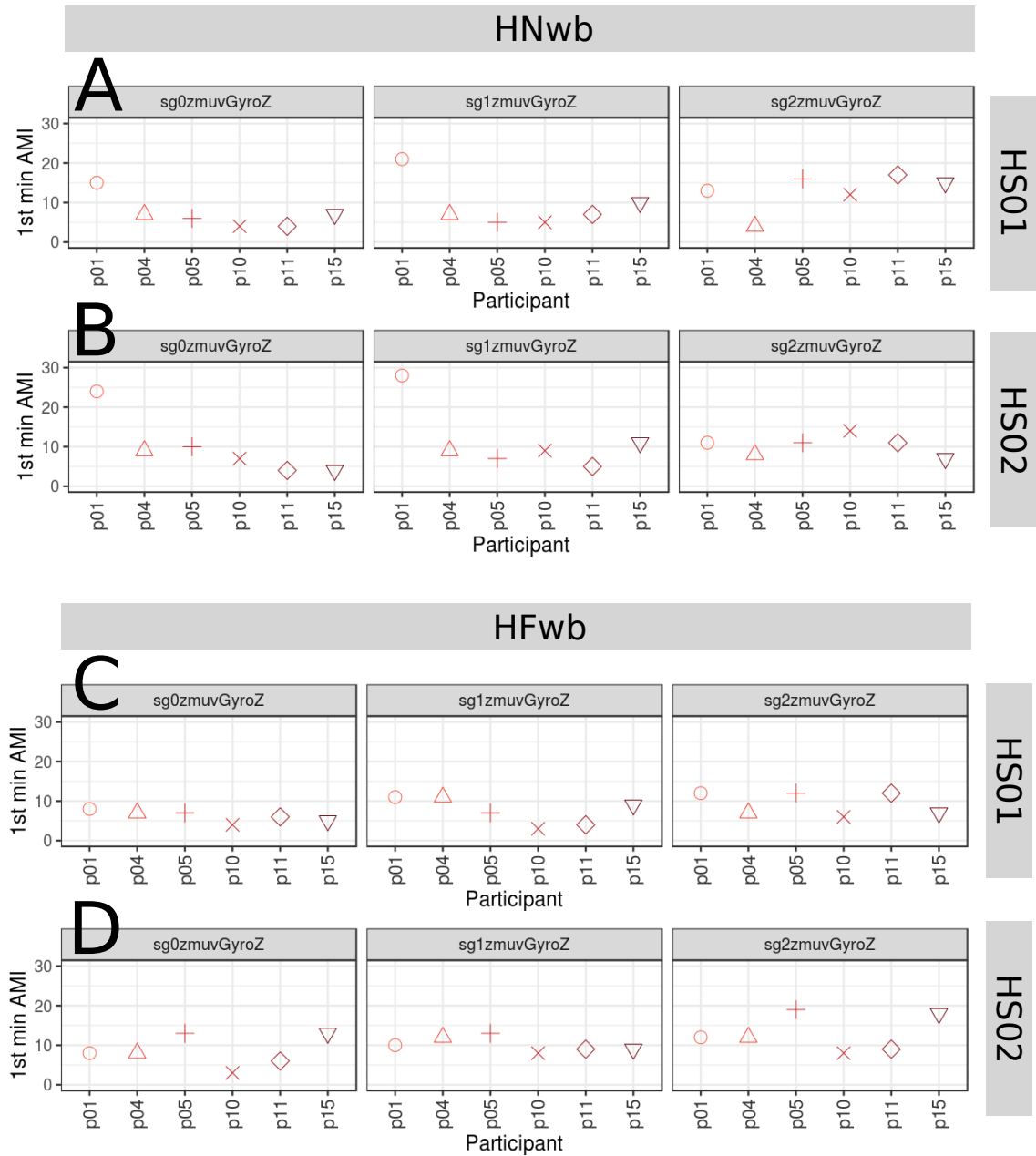


Fig. 5.10 **First minimum AMI values for horizontal arm movements (with beat).** (A, B) Horizontal Normal with beat (HNwb), and (C, D) Horizontal Faster with beat (HFwb) movements. (A, C) Sensor attached to the participant (HS01), and (B, D) sensor attached to the participant (HS02). First minimum AMI values are for six participants (p01, p04, p05, p10, p11, p15) with three smoothed signals (sg0zmuvGyroZ, sg1zmuvGyroZ and sg2zmuvGyroZ) and window lenght of 10-sec (500 samples). R code to reproduce the figure is available from Xochicale (2018).

Quantifying Human-Image Imitation Activities

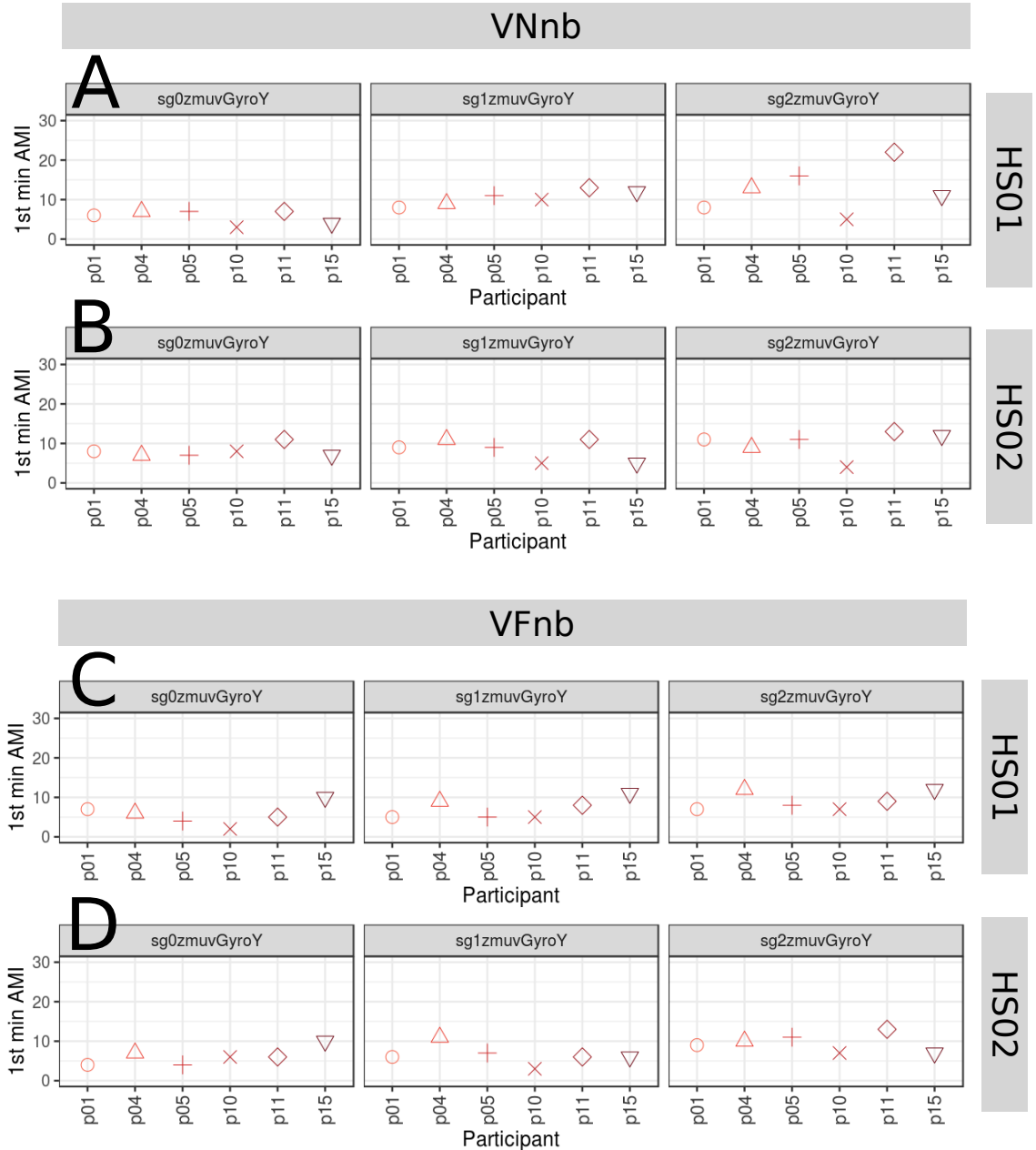


Fig. 5.11 **First minimum AMI values for vertical arm movements (no beat).** (A, B) Vertical Normal with no beat (VNnb), and (C, D) Vertical Faster with no beat (VFnb) movements. (A, C) Sensor attached to the participant (HS01), and (B, D) sensor attached to the participant (HS02). First minimum AMI values are for six participants (p01, p04, p05, p10, p11, p15) with three smoothed signals (sg0zmuvGyroZ, sg1zmuvGyroZ and sg2zmuvGyroZ) and window lenght of 10-sec (500 samples). R code to reproduce the figure is available from Xochicale (2018).

5.3 Minimum Embedding Parameters

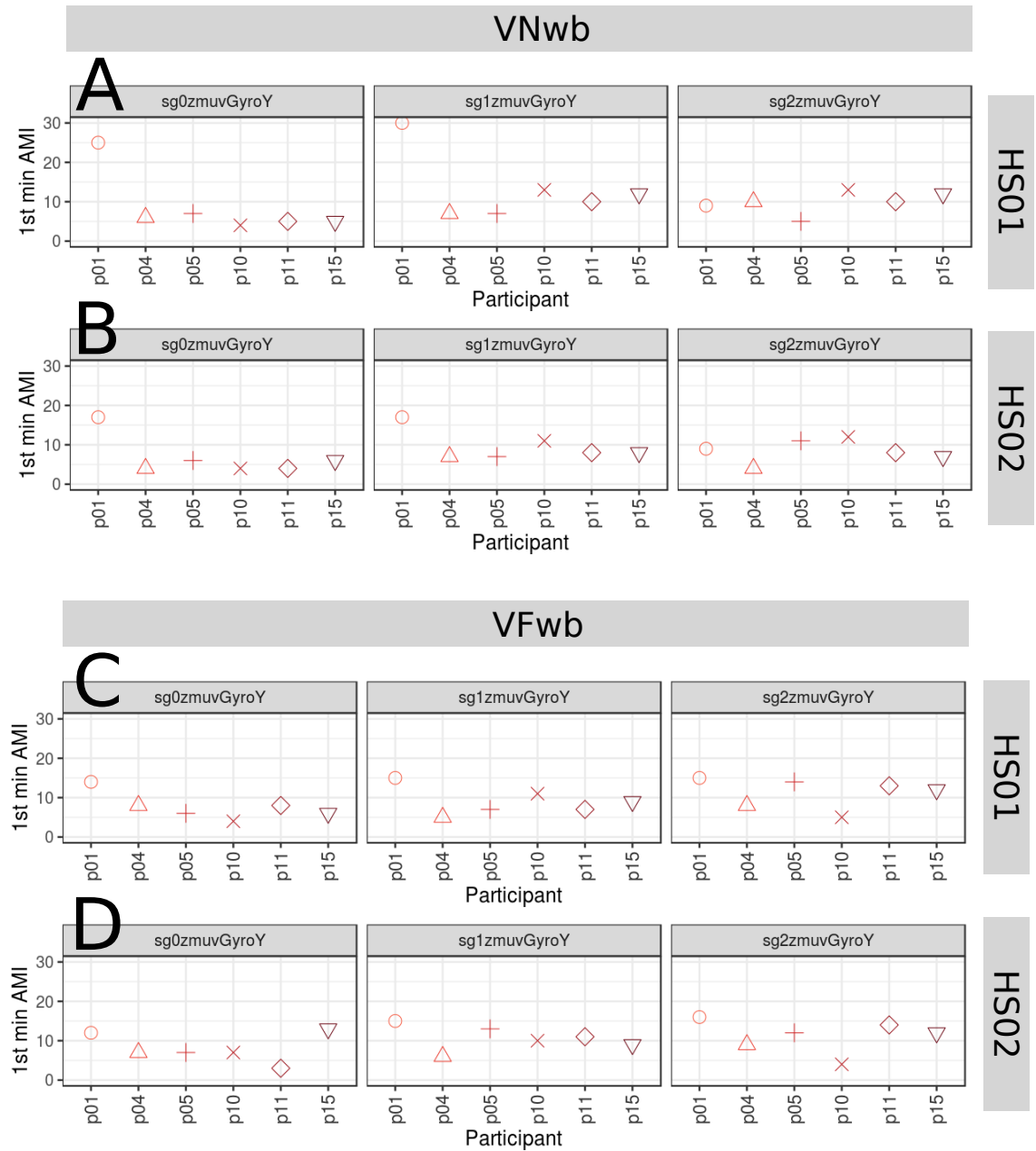


Fig. 5.12 First minimum AMI values for vertical arm movements (with beat). (A, B) Vertical Normal with beat (VNwb), and (C, D) Vertical Faster with beat (VFwb) movements. (A, C) Sensor attached to the participant (HS01), and (B, D) sensor attached to the participant (HS02). First minimum AMI values are for six participants (p01, p04, p05, p10, p11, p15) with three smoothed signals (sg0zmuvGyroZ, sg1zmuvGyroZ and sg2zmuvGyroZ) and window lenght of 10-sec (500 samples). R code to reproduce the figure is available from Xochicale (2018).

5.3.3 Average minimum embedding parameters

The average minimum embedding parameters is computed with a sample mean of $\bar{m}_0 = 9$ from the minimum values of $E_1(m)$ of Figs 5.5, 5.6, 5.7, and 5.8 and a sample mean of $\bar{\tau}_0 = 6$ from minimum values of AMIs of Figs 5.9, 5.10, 5.11, and 5.12 (Section 3.4.3). Hence, Reconstructed State Spaces (RSSs), Recurrence Plots (RPs), and Recurrence Quantification Analysis (RQA) metrics are computed with the average minimum embedding parameters ($\bar{m}_0 = 9$, $\bar{\tau}_0 = 6$).

5.4 Reconstructed state spaces with UTDE

Reconstructed state spaces for horizontal normal and horizontal faster arm movements with no beat are shown in Fig 5.13. The smoothness of the time series show a slightly change of smoothed trajectories in the RSSs for sg0zmuvGyroZ and sg1zmuvGyroZ, while the RSSs trajectories for sg2zmuvGyroZ appear to be distorted (Fig 5.13). One can see slightly differences in the RSSs trajectories when comparing sensors HS01 and HS02 for horizontal normal arm movement with no beat (Fig 5.13(A, B)) and horizontal faster arm movements with no beat (Fig 5.13(C, D)). With regards to the type of movement, the RSSs trajectories appear to change little when comparing horizontal normal with faster arm movements (Fig 5.13).

Fig 5.14 shows trajectories of the reconstructed state space for horizontal normal and horizontal faster arm movements while beat sounds. Hence, as in Fig 5.13, it can also be noted in Fig 5.14 that the smoothness of sg0zmuvGyroZ and sg1zmuvGyroZ appear to affect little the RSSs trajectories, while RSSs trajectories for sg2zmuvGyroZ substantially change so as to show different patterns. However, the trajectories in the RSS appear to change little when comparing the differences between the type of sensors

HS01 and HS02 (Fig 5.14). For the type of movements, trajectories show differences for horizontal normal and horizontal faster arm movements (Fig 5.14).

Fig 5.15 show trajectories for reconstructed state spaces of vertical normal and vertical faster arm movements with no beat. Smoothness of the RSSs trajectories is slightly noticed for sg0zmuvGyroY and sg1zmuvGyroY, whereas RSSs trajectories for sg2zmuvGyroY are evidently different (Fig 5.15). When comparing the RSSs trajectories from sensors HS01 and HS02, it can be noted little change, whereas the comparison from type of movement, the trajectories difference is more notable (Fig 5.15).

Fig 5.16 show trajectories for reconstructed state space of vertical normal and vertical faster arm movements for participants hearing a beat. Smoothness of RSSs trajectories appear to show slightly differences between sg0zmuvGyroY and sg1zmuvGyroY, however RSSs trajectories for sg2zmuvGyroY are different (Fig 5.16). With regards to the type of sensor HS01 and HS02, RSSs trajectories appear to change little, whereas for type of activity of normal and faster arm movements, RSSs trajectories show evidently differences (Fig 5.16).

5.5 Recurrences Plots

Considering the embedding parameters $m = 9$, $\tau = 6$ and a recurrence threshold $\epsilon = 1$, we present in this section recurrence plots (RPs) for participant $p01$ for horizontal and vertical arm movements in normal and faster velocity with beat and no beat sound (Figs 5.17, 5.18, 5.19 and 5.20).

Figs 5.17 show recurrence plots for horizontal normal and horizontal faster arm movements with no beat sound. For horizontal normal arm movements with no beat, patterns in RPs for sg0zmuvGyroZ and sg1zmuvGyroZ look similar, however patterns in RPs for sg2zmuvGyroZ are different (Figs 5.17), such behavior of RPs patterns

Quantifying Human-Image Imitation Activities

is similar with regards to the smoothness presented in horizontal and faster arm movements with beat (Fig 5.18). With regards to the type of sensor, there is little visual differences in RPs patters, while patterns of RPs for different activities present diagonal lines that appear to be closer and more dense with horizontal faster than horizontal normal arm movements (Fig 5.17).

Figs 5.18 show patterns of RPs for horizontal normal and faster arm movements while participants hear a beat. For these patterns in the RPs, the type activities for normal and faster arm movements can be easily noticed in the patterns, as well as the change of smoothness between sg0zmuvGyroZ and sg1zmuvGyroZ with the patterns for sg2zmuvGyroZ. It can also noted that there is little visual differences between the RP patters for sensor HS01 and HS02 (Figs 5.18).

Figs 5.19 show patterns of RPs for vertical normal and faster arm movements while no hearing a beat. One can note the the evidently differences of patterns between the levels of smoothness where, for instance, patterns of RPs from sg0zmuvGyroY and sg1zmuvGyroY looks similar while RPs for sg2zmuvGyroY are completely black. Similarly, one can see little visual changes when comparing RPs patterns between sensors HS01 and HS02. However, the RPs patterns create a more dense presence of diagonal lines for faster arm movements than normal arm movements (Figs 5.19).

Figs 5.20 show RPs patterns for vertical normal and faster arm movements for participants hearing a beat. Patterns of RP for vertical normal and vertical faster arm movements are visually noticeable as well as the RPs patterns for changes in the increase of smoothness between sg0zmuvGyroY and sg1zmuvGyroY and with sg2zmuvGyroY. Once can also note that there is little visual changes of RPs patterns from different sensors (Figs 5.20).

5.6 Recurrence Quantification Analysis

In this section is shown Recurrence Quantification Analysis (RQA) metrics (REC, DET, RATIO and ENTR) for six participants ($p01, p04, p05, p10, p11, p15$) for horizontal arm movements (HNnb, HNwb, HFnb, HFwb) and vertical arm movements (VNnb, VNwb, VFnb, VFwb) for sensors HS01 and HS02 with three smoothed time series (sg0zmuvGyro, sg1zmuvGyro and sg2zmuvGyro).

5.6.1 REC values

Figs 5.21 and 5.22 show REC values, representing the % of black dots in the RPs, for vertical and horizontal arm movements.

It can be noted in Fig 5.21 that REC values present little differences when comparing sensor HS01 and HS02. Similarly, considering the smoothness of the time series, REC values for participants appear to be similar in each of the activities (HNnb, HNwb, HFnb, HFwb) for sg0zmuvGyroZ and sg1zmuvGyroZ, while REC values for sg2zmuvGyroZ appear to fluctuate a bit more. With regards to the type of activity, horizontal arm movements with beat (HNwb) appear to fluctuate more than other activities (HNnb, HFnb, HFwb). Also RET values appear to fluctuate more and be greater for faster arm movements whereas RET values for normal arm movements appear to be constant (Fig 5.21).

Figs 5.22 show RET values for vertical arm movements. It can be noted that RET values appear to be similar for sensors HS01 and HS02 and the smoothness effect in REC values is more evident for sg2zmuvGyroY than REC values for sg0zmuvGyroY and sg1zmuvGyroY. RET values appear to fluctuate more for vertical normal arm movements with beat (VNwb) than other activities (VNnb, VFnb, VFwb) and RET values for VNnb, VFnb and VFwb appear to be constant and show little fluctuation between participants.

5.6.2 DET values

DET values, representing predictability and organisation of the RPs, appear to be constant for any source of time series (Figs 5.23 and 5.24). For both horizontal and vertical arm movements, the increase of smoothness of time series appear to affect the smoothness of DET values by making them to appear more similar as the smoothness increase. Additionally, it can be noted more fluctuations of DET values for faster activities (HFnb, HFwb) than normal activities (HNnb, HNwb), specifically for sg0zmuvGyroY (Figs 5.23, 5.24).

5.6.3 RATIO values

RATIO values, representing dynamics transitions, for horizontal and vertical arm movements are shown in Figs 5.25 and 5.26.

The fluctuation of RATIO values for horizontal faster arm movements appear to be more notable than RATIO values for horizontal normal arm movements. RATIO values appear to be constant for activity HNwb than other activities (HNnb, HFnb, HFwb). Regarding the smoothness of time series, RATIO values appear to have similar values for sg0zmuvGyroZ and sg1zmuvGyroZ while RATIOS values are more uniform for sg2zmuvGyroZ. With regards to type of sensor, RET values appear to be similar for HS01 and HS02 with the exception of *p15* in HFnb activity (Figs 5.25).

Figs 5.26 show RATIO values for vertical arm movements. The fluctuation of RATIO values appears to be constant for the activity VNwb whereas other RATIO values for other activities (VNnb, VFnb, VFwb) appear to fluctuate more. The smoothness of the time series affects only the RATIO values for sg2zmuvGyroY as these appear to be constant, while RET values for sg0zmuvGyroY and sg1zmuvGyroZ appear to have the similar RATIO values. Additionally, RATIO values for type of sensors HS01 and HS02 appear to show similar values as well, with the exception of *p15* in the VFnb activity.

5.6.4 ENTR values

ENTR values, representing the complexity of the deterministic structure of time series, for horizontal and vertical arm movements are shown in Figs 5.27 and 5.28.

Figs 5.27 show ENTR values for horizontal arm movements. ENTR values appear to be similar for sg0zmuvGyroZ and sg1zmuvGyroZ and oscillate between 2 to 4, while ENTR values for sg2zmuvGyroZ appear to show similar fluctuations but with higher ENTR values oscillating between 3.5 to 5 with the exception of p_{10} with activities VNnb and VFwb for sg2zmuvGyroY which ENTR values are slightly out of range. ENTR values appear to be similar for sensor HS01 and HS02.

Figs 5.28 show ENTR values for vertical arm movements. ENTR values for sg0zmuvGyroY and sg1zmuvGyroY appear to show the same values and oscillate between 2 to 4, while ENTR values appear to oscillate between 3.5 to 5 with the exception of p_{10} with activities VNnb and VFwb for sg2zmuvGyroY which ENTR values are out of range. ENTR values for sensor HS01 and HS02 appear to show the same values.

5.7 The weaknesses and strengths of RQA

Surfaces for RQA metrics (REC, DET, RATIO, ENTR) are computed with the variation of embedding values by an increase of one ($0 \geq m \leq 10$, $0 \geq \tau \leq 10$) and recurrence thresholds by an increase of 0.1 ($0.2 \geq \epsilon \leq 3$). Hence, we show different characteristics of 3D surfaces of RQA considering different activities, sensors, window size lengths and level of smoothness and participants.

Figs 5.29 show the surfaces for RQA metrics (REC, DET, RATIO, ENTR) using time series of participant p_{01} , sensor HS01, activity HNnb, sg0zmuvGyroZ axis and a 500 window size length. The 3D surface for REC values, representing the % of

Quantifying Human-Image Imitation Activities

recurrence dots in the RP, show highest values of REC when embedding values are near to 1 and the recurrence threshold is at the maximum ($\epsilon = 3$ for this surfaces). Similarly, it can be seen a decrease of REC values as the embedding dimension and embedding delay values increase, however there is an increase of REC values as the recurrence threshold is increasing (Fig 5.29(A)). Regarding the 3D surface for DET values, representing predictability and organisation of the RPs, Fig 5.29(B) show slightly uniform values when varying both embedding parameters and recurrence threshold with the exception of embedding parameters near to 1 and recurrence thresholds near to 0.2 where the DET values are smaller. 3D surface for RATIO values, representing dynamic transitions, show a plateau with low values recurrence threshold values greater than 1.0. However, there is a fluctuated increase of RATIO values as the embedding values increase given that the recurrence threshold is lower than 1 (Fig 5.29(C)). For ENTR values, representing the complexity of the structure of the time series, Fig 5.29(D) show a maximum value of ENTR when embedding parameters are near to 1 and recurrence threshold values are near to 3.0. It can also be noted fluctuations in the 3D surface when ENTR values are greater than 2.5 (red surface) for embedding dimensions between 3 to 9 and a decrease of ENTR values per each embedding dimension for delay embedding values (yellow surface). Additionally, ENTR values decrease as the embedding dimension and delay embedding decrease.

5.7.1 Sensors and activities

Figs 5.30 and 5.31 show 3D surfaces of RQA metrics (REC, DET, RATIO, ENTR) for horizontal arm movements (HNnb, HNwb, HFnb, HFwb) using sensor HS01 and HS02 for participant *p01* with sg0zmuvGyroZ axis and 500 window size lenght. Hence, Figs 5.30 present 3D surfaces of RQA metrics for HS01, where 3D surfaces for REC values (Fig 5.30(A)) appear to be similar across the activities (HNnb, HFnb, HFwb)

5.7 The weaknesses and strengths of RQA

with the exception of HNwb which decrease of REC values is mainly affected by the increase of recurrence threshold and slightly affected to the increase of embedding dimension parameters. For DET values, 3D surfaces in Figs 5.30(B) appear to show values near to 1.0 (red colour surface), however HNwb shown fluctuations of DET values as the embedding dimension increase, it can also be noted a decrease of DET values for certain values of recurrence threshold (2.6 for HNwb, 0.3 for HFnb, and 0.3 for HFwb). For Fig 5.30(C)), 3D surfaces for RATIO values appear to be similar, showing a plateau for values between 0 to 50 (blue surface) and the increase of peaks is different for each of the activities. For Fig 5.30(D), ENTR values present different surface formations, for instance, HNnb show fluctuated higher values of ENTR (red colour surface), whereas for activity HNwb the ENTR values are higher (red colour surface) for recurrence threshold near to 3.0, ENTR values for HFnb appear to be higher when embedding dimension is near to 10, while higher values for ENTR values for HFwb appear to be when the recurrence threshold is near to 0.2.

Then, looking and comparing visually one by one of the surfaces for sensors HS01 and HS02 in Figs 5.30 and 5.31, one can notice little differences in the shape of the surfaces. Similarly, there is little variations in the surfaces for vertical arm movements with the sensors HS01 and HS02 (Figs 5.32 and 5.33).

With regards to horizontal and vertical movements, 3D surfaces appear to be similar for REC, DET and RATIO values with sensor HS01 (Figs 5.30 and 5.32) and sensor HS02 (Figs 5.31 and 5.33), however 3D surfaces for ENTR values in each of the arm movements presents distinguishable variations in the surfaces, see Figs 5.30(D) and 5.32(D) for horizontal and vertical arm movements with sensor HS01 and Figs 5.31(D) and 5.33(D) for horizontal and vertical arm movements with sensor HS02.

Quantifying Human-Image Imitation Activities

5.7.2 Window size

3D surfaces of REC values with a short window length (100 samples) can affect the shape of 3D surface, however for window size of 250, 500, and 700 samples, the 3D surfaces appear to show little changes (Figs 5.34(A)). For instance, one can see 3D surfaces of DET values with a window of 100 size length is slightly different to other surfaces but keeping the plateau (red surface) in each of the surfaces (Figs 5.34(B)). Similarly, the 3D surfaces of RATIO values preserve the same plateau (blue surface) with little variations in the surfaces as window size length increase (Figs 5.34(C)). 3D surfaces for ENTR values appear to have similar aspects as the fluctuations of the curves keeps the same values (red and yellow colours). It can also be noted that the smoothness of 3D surfaces decrease as the embedding dimension parameters increase and such smoothness is also affected by the window length (see Figs 5.34(D)).

5.7.3 Smoothness

Figs 5.35 show the effects of three levels of smoothness ($sg0zmuvGyroZ$, $sg1zmuvGyroZ$ and $sg2zmuvGyroZ$) in the RQA metrics. Generally, 3D surfaces from $sg2zmuvGyroZ$ are affected by the smoothness. It can also be noted that REC values and ENTR values present a slightly different surfaces (see Figs 5.35(A, D)), while DET and RATIO values appear to be similar which is mainly reflected in the colour of the curves (see Figs 5.35(B, C)). In Figs 5.35(A), 3D surfaces for REC values tend be smoothed as the smoothness of the time series increase to the point where the increase of recurrence threshold affects the shape of the surfaces. Similarly, in Figs 5.35(C), 3D surface for ENTR values is affected by the smoothness of the time series to the point that the fluctuations in the surface does change drastically the shape by showing only an increase of ENTR values as the recurrence threshold increase.

5.7.4 Participants

The shape of 3D surfaces of RQA metrics is also affected when using time series from different participants (Figs 5.36). For instance, 3D surface of DET values show slightly but noticeable differences in the fluctuations when embedding dimension and recurrence threshold increase (Figs 5.36(B)) which is similar for ENTR values where the fluctuations of the 3D surfaces changes for each of the participants (Figs 5.36(D)). However, the shape of 3D surfaces for RET values and RATIO values is little affected with the change of participants (Figs 5.36(A, C)).

5.7.5 Final remarks

Independently of the source of time series, surfaces for RATIO values are affected little by the changes of embedding values and recurrence thresholds with the exception for the peaks presented when embedding values increase for recurrence thresholds less than one. Then, 3D surfaces for DET values are affected slightly more than RATIO values and the changes are also independent of the source of time series. Nonetheless, REC values are affected by the window size, type of activity and level of smoothness. For ENTR values, we can see that 3D surfaces show clearly differences with regards to any of the sources of the time series, hence making ENTR metric a robust metric to quantify human movement variability from different time series.

Quantifying Human-Image Imitation Activities

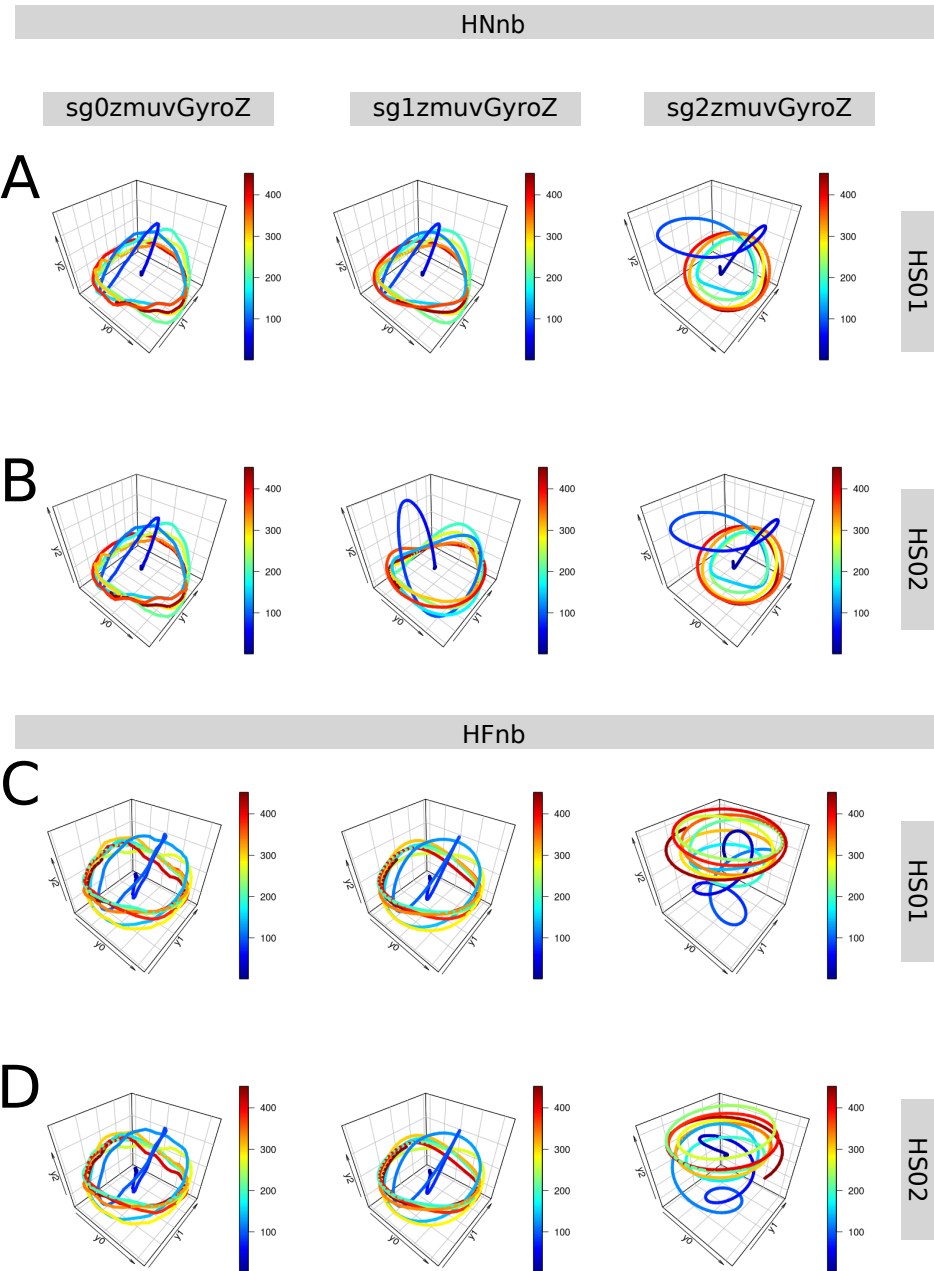


Fig. 5.13 RSSs for horizontal arm movements (no beat). Reconstructed state spaces of participant p01 for (A, B) horizontal normal movements with no beat (HNnb) and (C, D) horizontal faster velocity with no beat (HFnb). Time series for raw-normalised (sg0zmuvGyroZ), normalised-smoothed 1 (sg1zmuvGyroZ) and normalised-smoothed 2 (sg2zmuvGyroZ) with (A, C) sensor attached to the participant (HS01), and (B, D) sensor attached to the participant (HS02). Reconstructed state spaces were computed with embedding parameters $m = 9$, $\tau = 6$. R code to reproduce the figure is available from Xochicale (2018).

5.7 The weaknesses and strengths of RQA

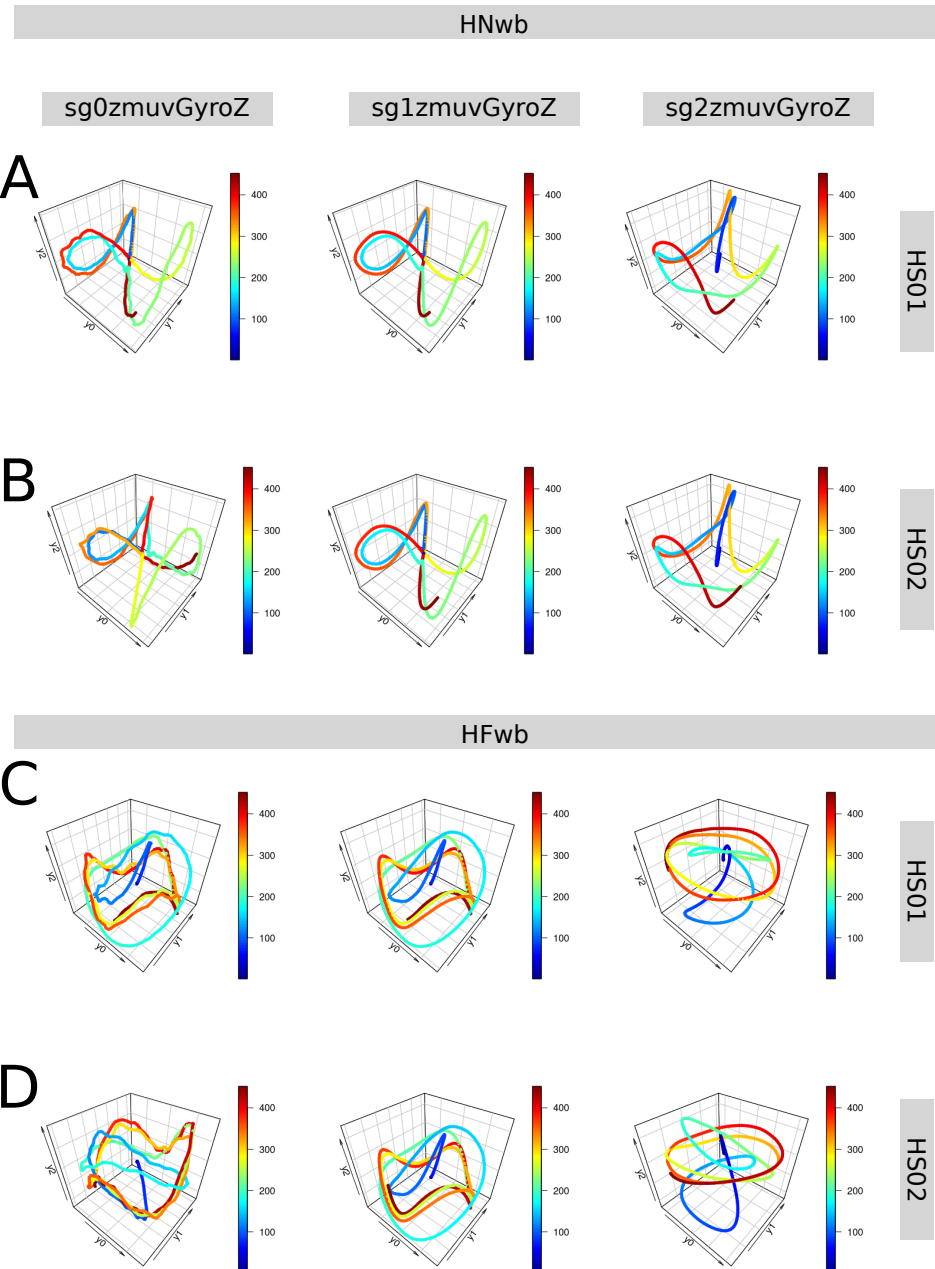


Fig. 5.14 RSSs for horizontal arm movements (with beat). Reconstructed state spaces of participant p01 for (A, B) horizontal normal movements with beat (HNwb) and (C, D) horizontal faster velocity with beat (HFwb). Time series for raw-normalised ($sg0zmuvGyroZ$), normalised-smoothed 1 ($sg1zmuvGyroZ$) and normalised-smoothed 2 ($sg2zmuvGyroZ$) with (A, C) sensor attached to the participant (HS01), and (B, D) sensor attached to the participant (HS02). Reconstructed state spaces were computed with embedding parameters $m = 9$, $\tau = 6$. R code to reproduce the figure is available from Xochicale (2018).

Quantifying Human-Image Imitation Activities

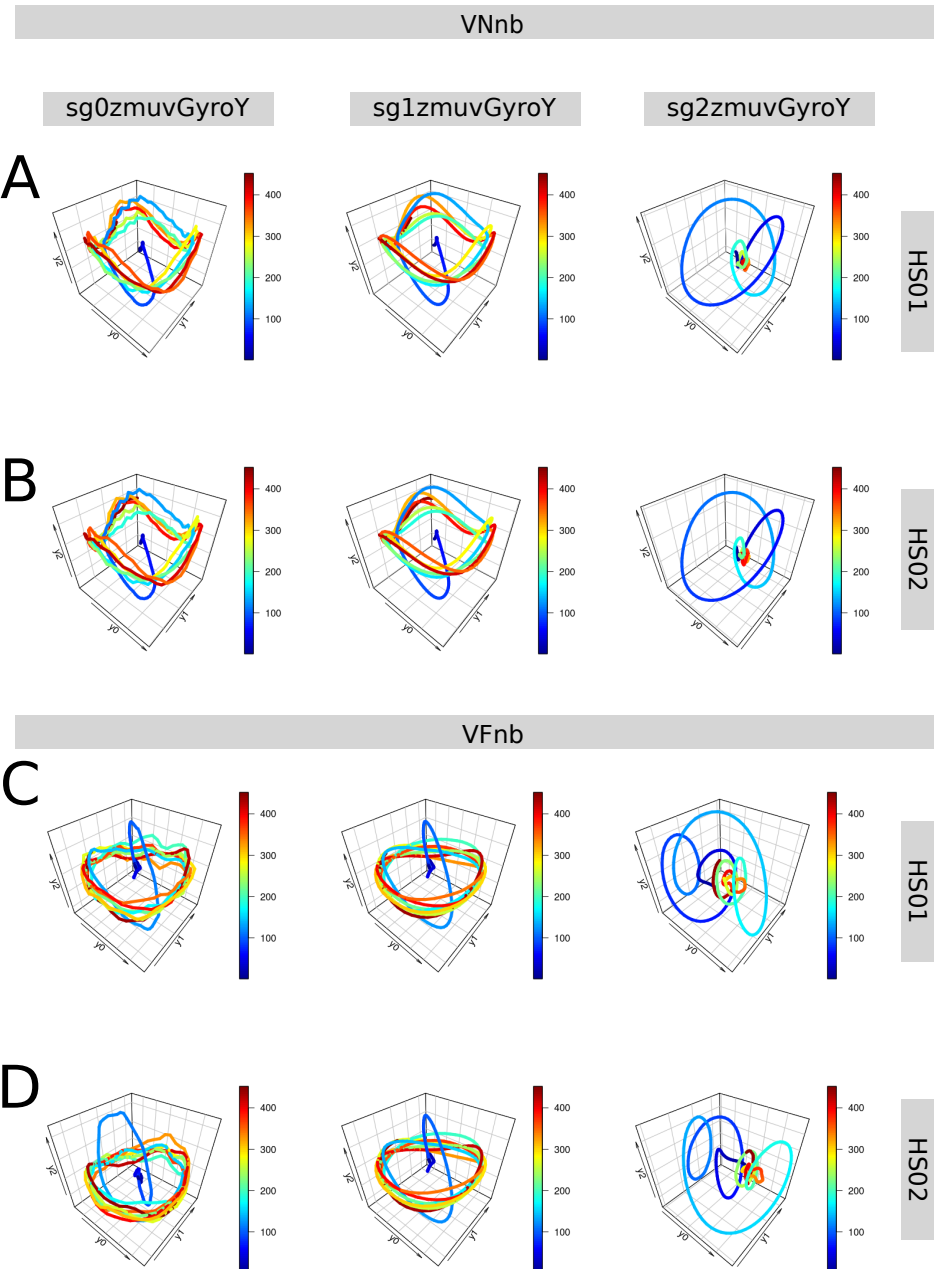


Fig. 5.15 RSSs for vertical arm movements (no beat). Reconstructed state spaces of participant p01 for (A, B) vertical normal movements with no beat (VNnb) and (C, D) vertical faster velocity with no beat (VFnb). Time series for raw-normalised ($sg0zmuvGyroY$), normalised-smoothed 1 ($sg1zmuvGyroY$) and normalised-smoothed 2 ($sg2zmuvGyroY$) with (A, C) sensor attached to the participant (HS01), and (B, D) sensor attached to the participant (HS02). Reconstructed state spaces were computed with embedding parameters $m = 9$, $\tau = 6$. R code to reproduce the figure is available from Xochicale (2018).

5.7 The weaknesses and strengths of RQA

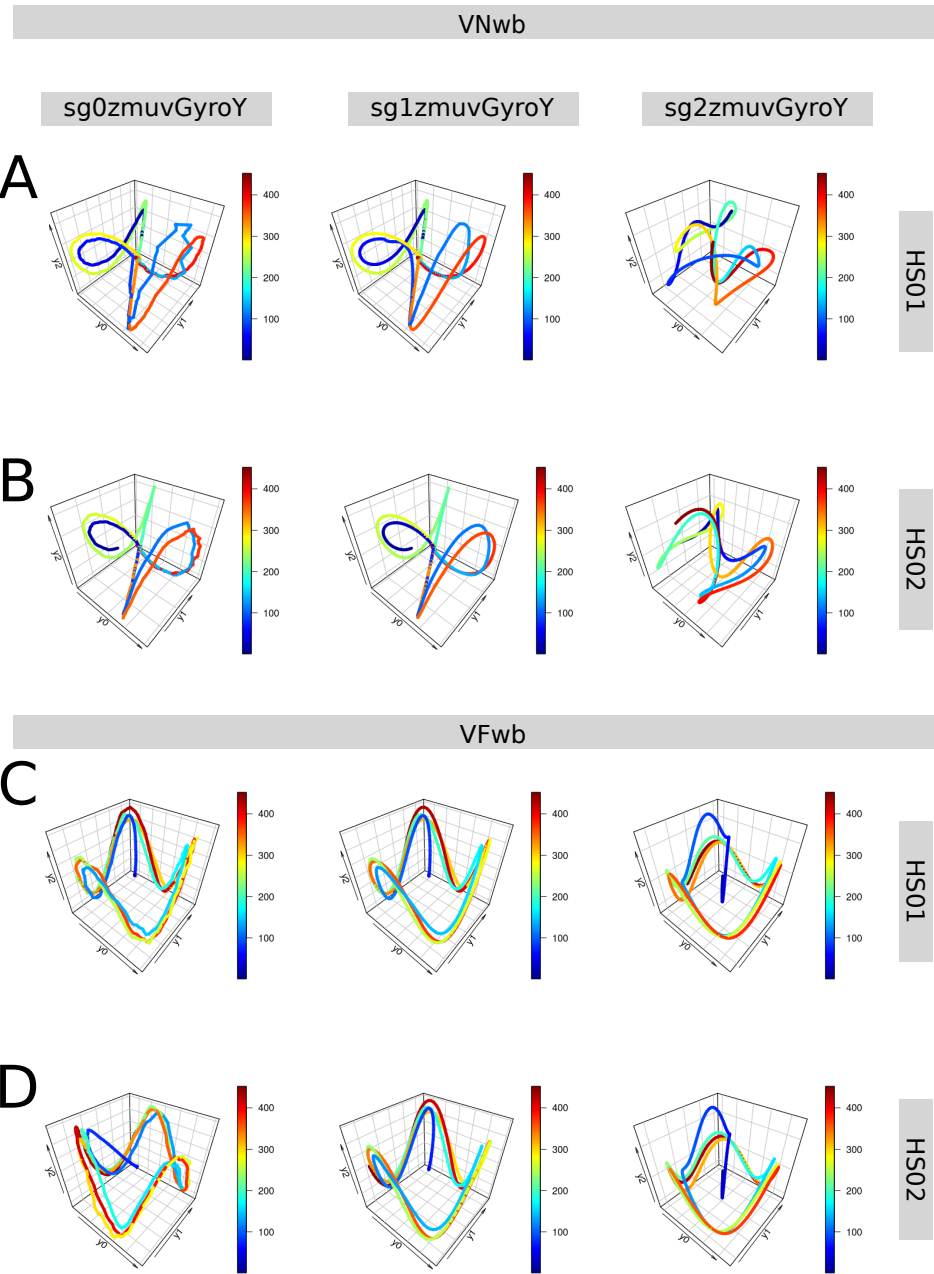


Fig. 5.16 **RSSs for vertical arm movements (with beat).** Reconstructed state spaces of participant p01 for (A, B) vertical normal movements with beat (VNwb) and (C, D) vertical faster velocity with beat (VFwb). Time series for raw-normalised ($sg0zmuvGyroY$), normalised-smoothed 1 ($sg1zmuvGyroY$) and normalised-smoothed 2 ($sg2zmuvGyroY$) with (A, C) sensor attached to the participant (HS01), and (B, D) sensor attached to the participant (HS02). Reconstructed state spaces were computed with embedding parameters $m = 9$, $\tau = 6$. R code to reproduce the figure is available from Xochicale (2018).

Quantifying Human-Image Imitation Activities

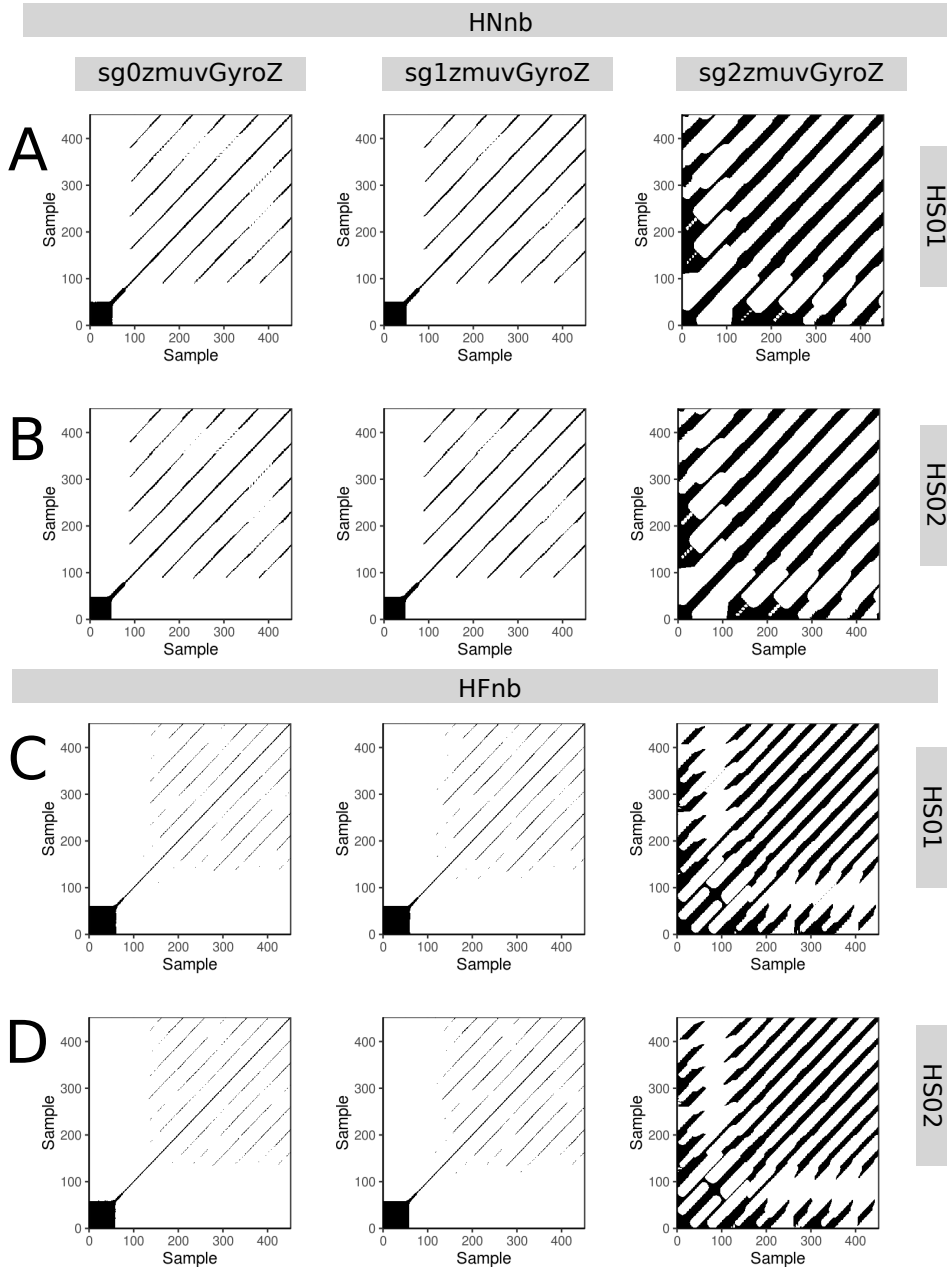


Fig. 5.17 RPs for horizontal arm movements (no beat). Recurrence plots of participant p01 for (A, B) horizontal normal movements with no beat (HNnb) and (C, D) horizontal faster movements with no beat (HFnb). Time series for raw-normalised ($sg0zmuvGyroZ$), normalised-smoothed 1 ($sg1zmuvGyroZ$) and normalised-smoothed 2 ($sg2zmuvGyroZ$) with (A, C) sensor 01 attached to the participant (HS01), and (B, D) sensor 02 attached to the participant (HS02). Recurrence plots were computed with embedding parameters $m = 9$, $\tau = 6$ and recurrence threshold $\epsilon = 1$. R code to reproduce the figure is available from Xochicale (2018).

5.7 The weaknesses and strengths of RQA

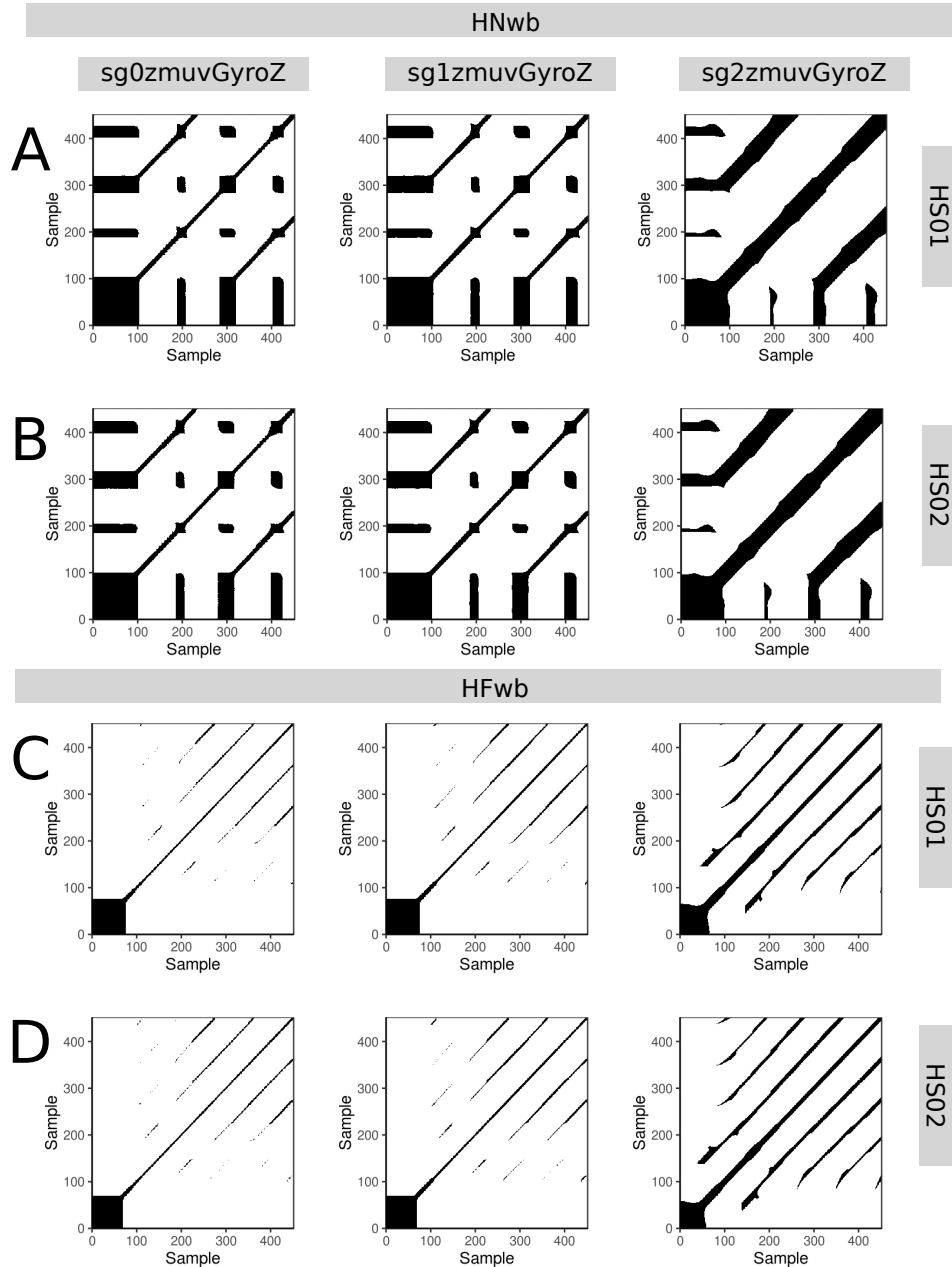


Fig. 5.18 **RPs for horizontal arm movements (with beat).** Recurrence plots of participant p01 for (A, B) horizontal normal movements with beat (HNwb) and (C, D) horizontal faster movements with beat (HFwb). Time series for raw-normalised ($sg0zmuvGyroZ$), normalised-smoothed 1 ($sg1zmuvGyroZ$) and normalised-smoothed 2 ($sg2zmuvGyroZ$) with (A, C) sensor 01 attached to the participant (HS01), and (B, D) sensor 02 attached to the participant (HS02). Recurrence plots were computed with embedding parameters $m = 9$, $\tau = 6$ and recurrence threshold $\epsilon = 1$. R code to reproduce the figure is available from Xochicale (2018).

Quantifying Human-Image Imitation Activities

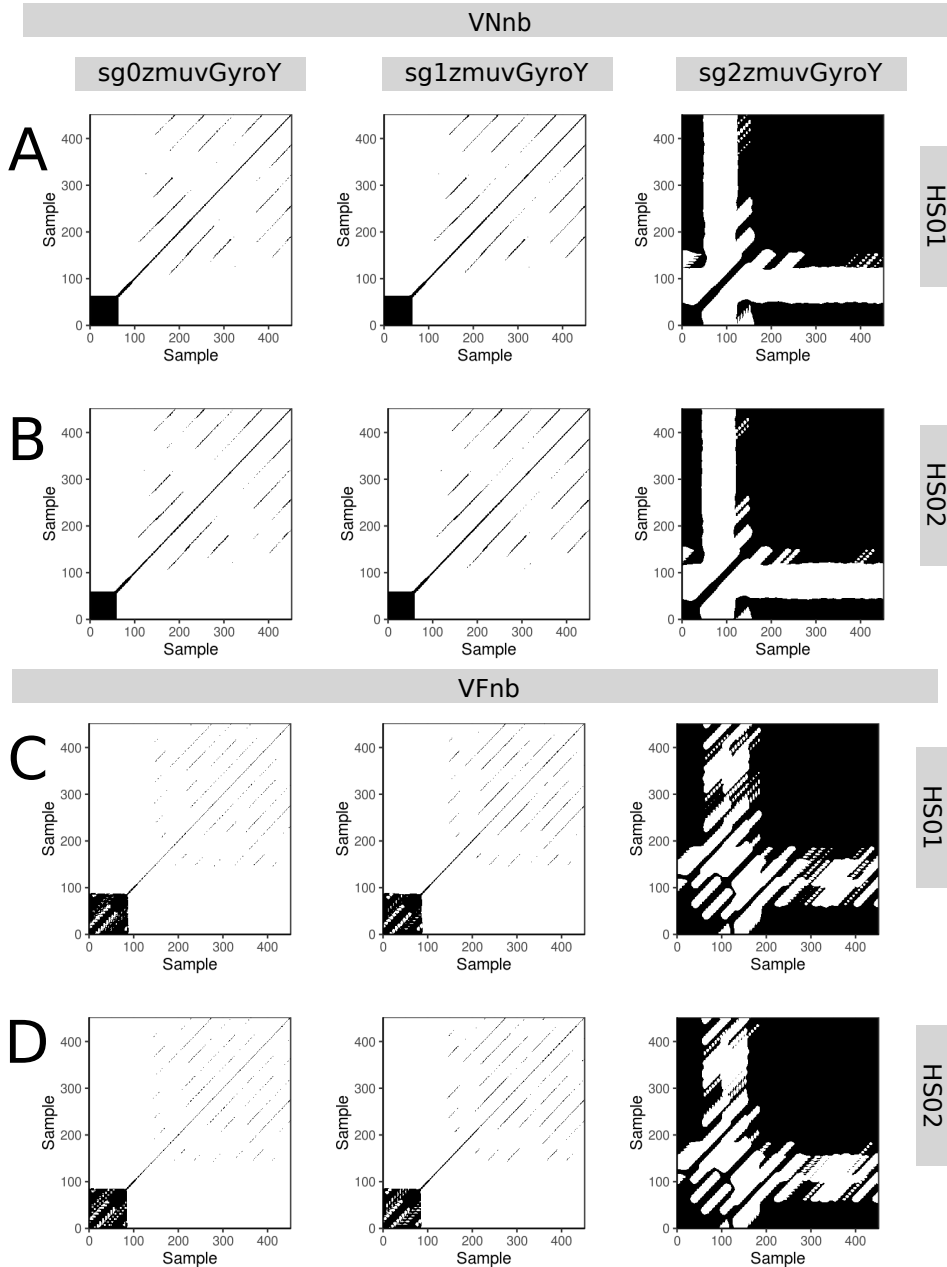


Fig. 5.19 RPs for vertical arm movements (no beat). Recurrence plots of participant p01 for (A, B) vertical normal movements with no beat (VNnb) and (C, D) vertical faster movements with no beat (VFnb). Time series for raw-normalised ($sg0zmuvGyroY$), normalised-smoothed 1 ($sg1zmuvGyroY$) and normalised-smoothed 2 ($sg2zmuvGyroY$) with (A, C) sensor 01 attached to the participant (HS01), and (B, D) sensor 02 attached to the participant (HS02). Recurrence plots were computed with embedding parameters $m = 9$, $\tau = 6$ and recurrence threshold $\epsilon = 1$. R code to reproduce the figure is available from Xochicale (2018).

5.7 The weaknesses and strengths of RQA

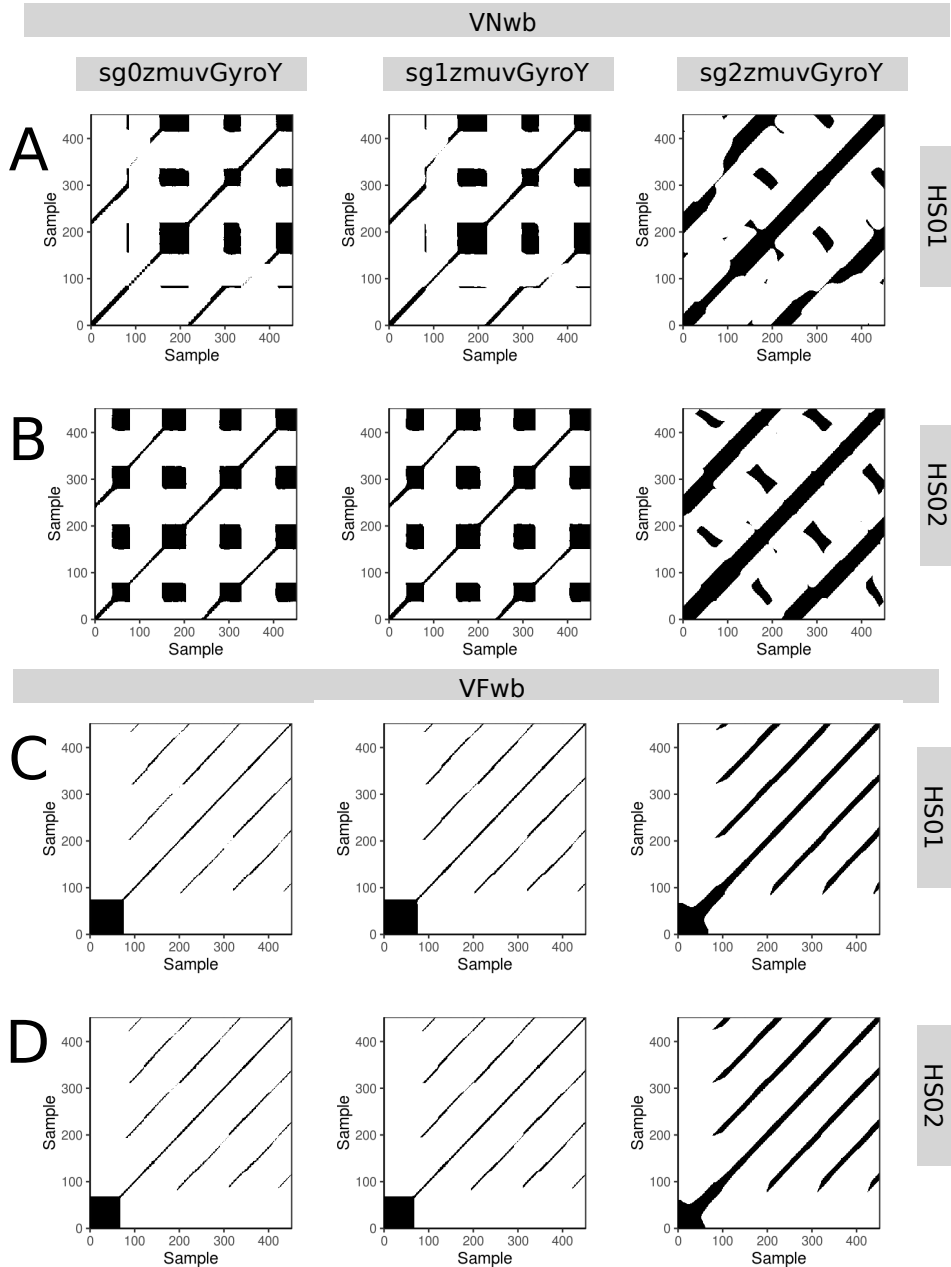


Fig. 5.20 RPs for vertical arm movements (with beat). Recurrence plots of participant p01 for (A, B) vertical normal movements with beat (VNwb) and (C, D) vertical faster movements with beat (VFwb). Time series for raw-normalised ($sg0zmuvGyroY$), normalised-smoothed 1 ($sg1zmuvGyroY$) and normalised-smoothed 2 ($sg2zmuvGyroY$) with (A, C) sensor 01 attached to the participant (HS01), and (B, D) sensor 02 attached to the participant (HS02). Recurrence plots were computed with embedding parameters $m = 9$, $\tau = 6$ and recurrence threshold $\epsilon = 1$. R code to reproduce the figure is available from Xochicale (2018).

Quantifying Human-Image Imitation Activities

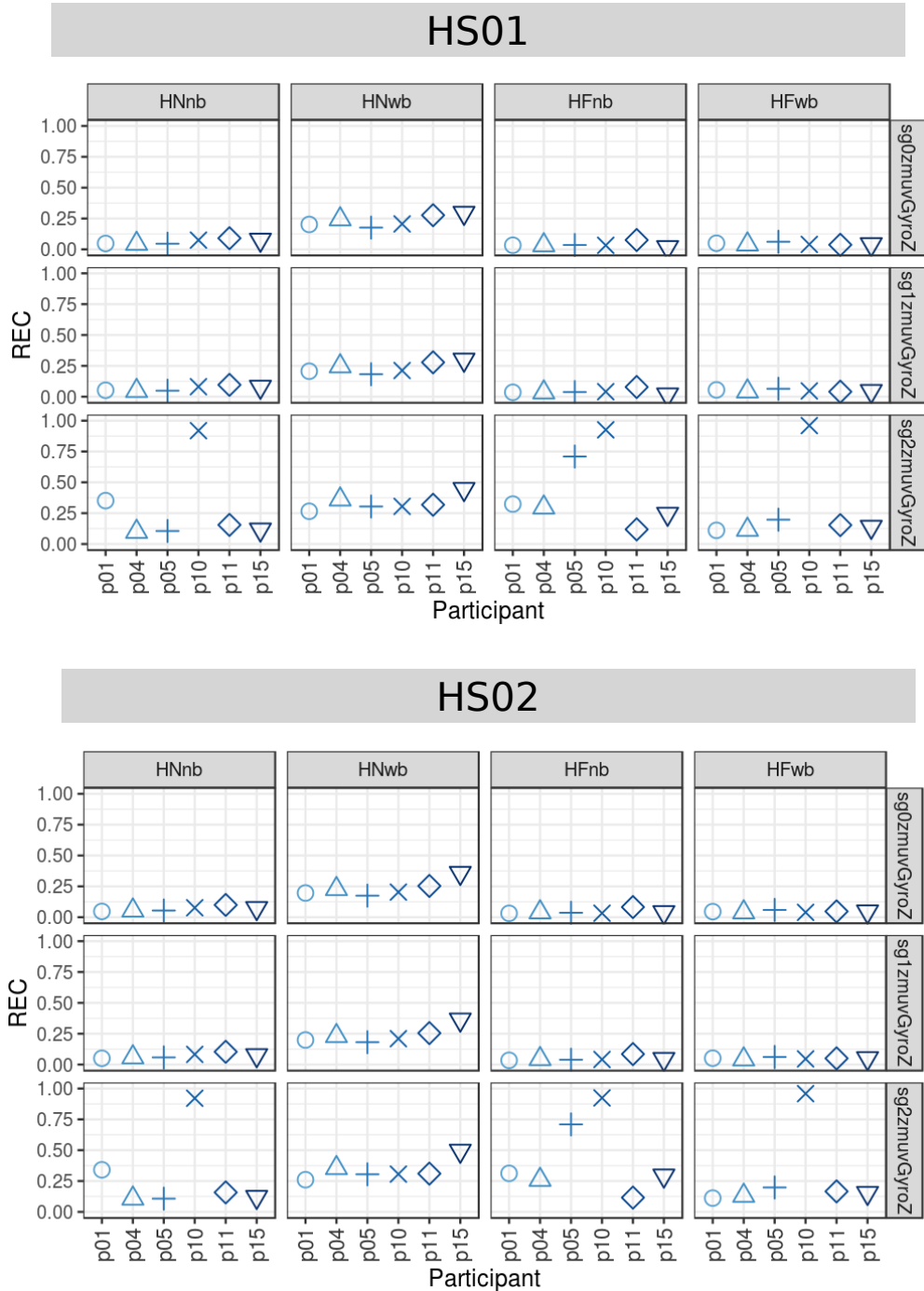


Fig. 5.21 **REC values for horizontal arm movements.** REC values (representing % of black dots in the RPs) for 6 participants performing horizontal arm movements (HNnb, HNwb, HFnb, HFwb) for sensors HS01, HS02 and three smoothed-normalised axis of GyroZ (sg0zmuvGyroZ, sg1zmuvGyroZ and sg2zmuvGyroZ). REC values were computed with embedding parameters $m = 9$, $\tau = 6$ and recurrence threshold $\epsilon = 1$. R code to reproduce the figure is available from Xochicale (2018).

5.7 The weaknesses and strengths of RQA

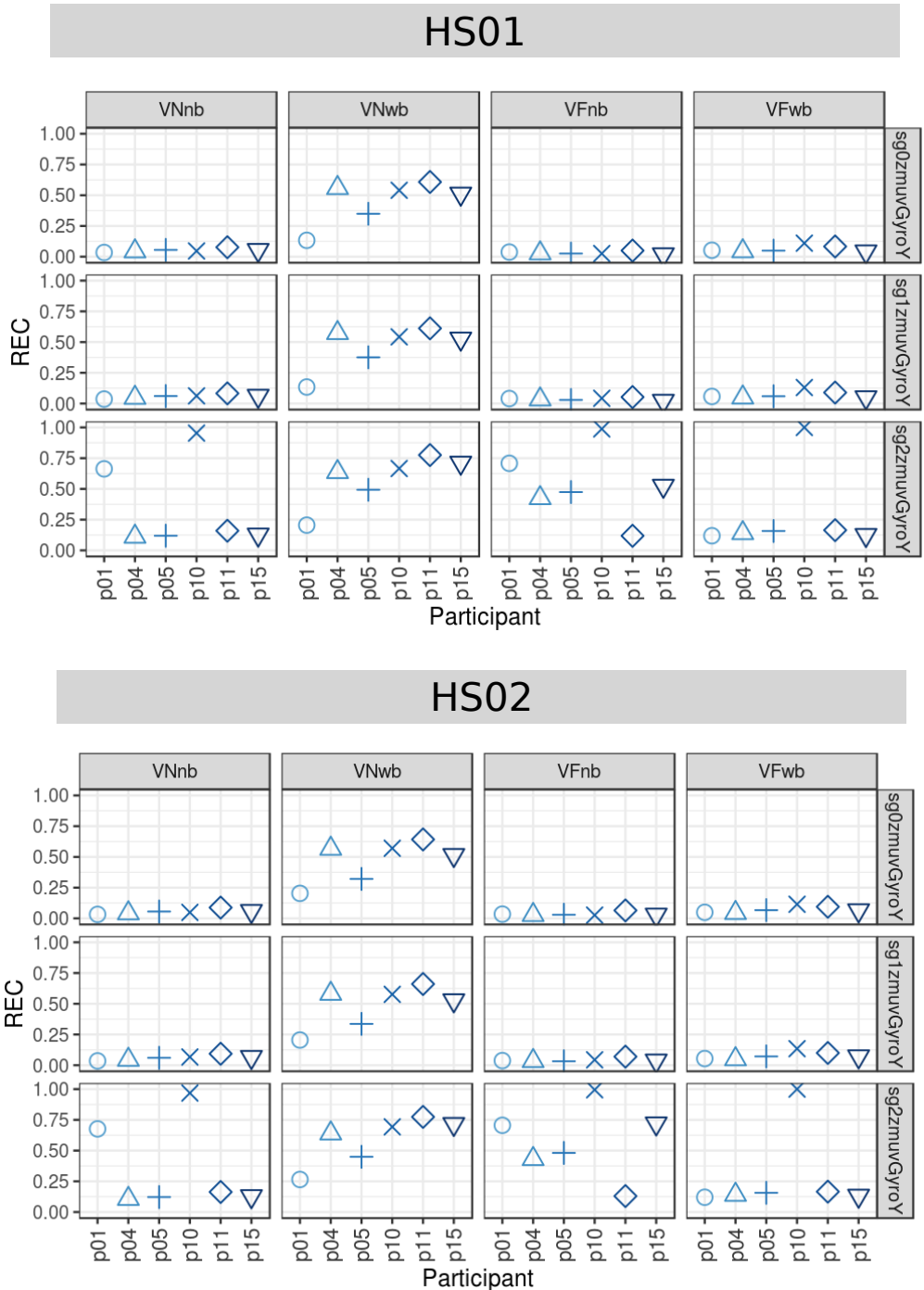


Fig. 5.22 REC values for vertical arm movements. REC values (representing % of black dots in the RPs) for 6 participants performing vertical arm movements (VNnb, VNwb, VFnb, VFwb) for sensors HS01, HS02 and three smoothed-normalised axis of GyroZ (sg0zmuvGyroZ, sg1zmuvGyroZ and sg2zmuvGyroZ). REC values were computed with embedding parameters $m = 9$, $\tau = 6$ and recurrence threshold $\epsilon = 1$. R code to reproduce the figure is available from Xochicale (2018).

Quantifying Human-Image Imitation Activities

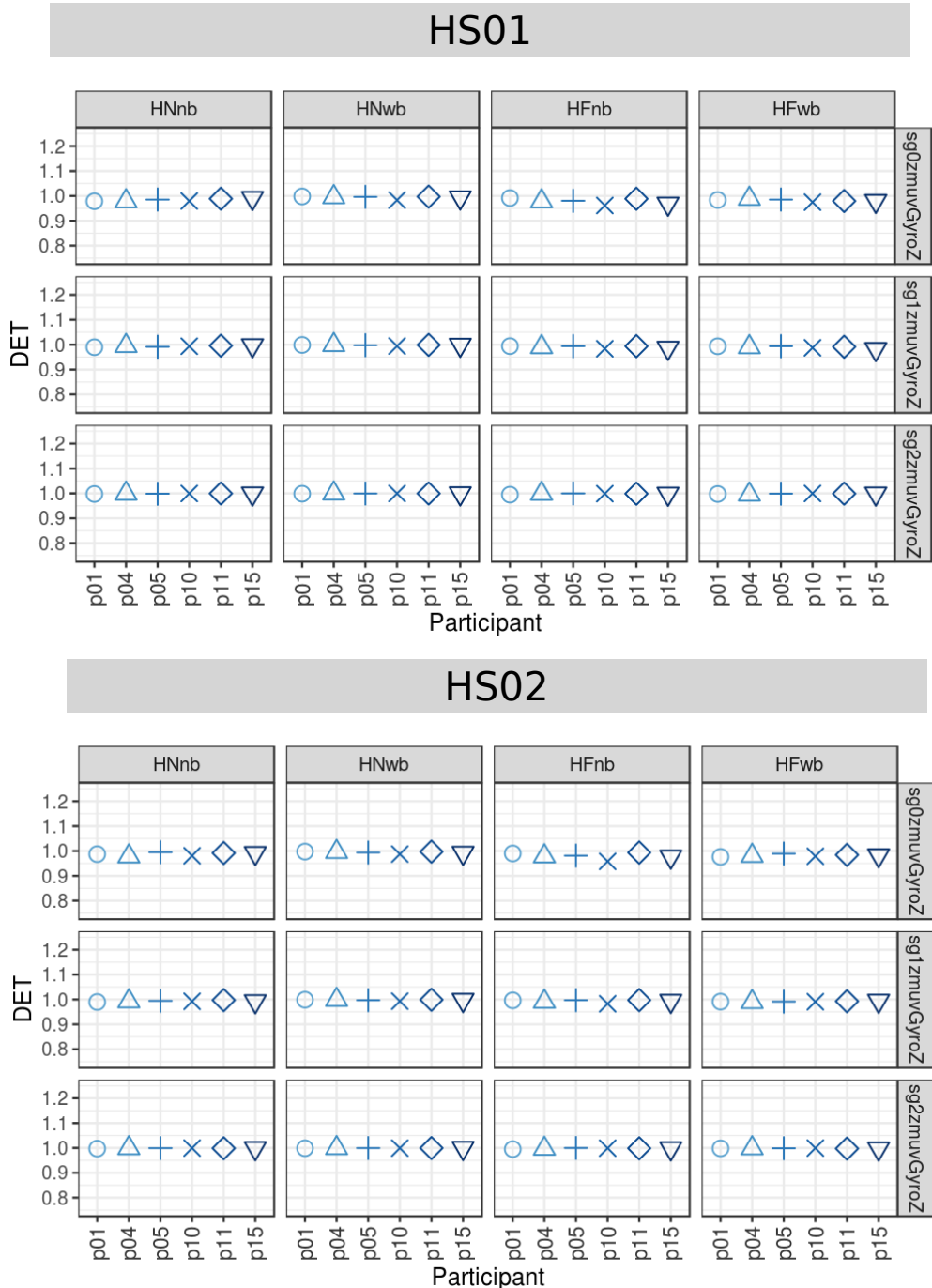


Fig. 5.23 **DET values for horizontal arm movements.** DET values (representing predictability and organisation of the RPs) for 6 participants performing horizontal arm movements (HNnb, HNwb, HFnb, HFwb) for sensors HS01, HS02 and three smoothed-normalised axis of GyroZ (sg0zmuvGyroZ, sg1zmuvGyroZ and sg2zmuvGyroZ). DET values were computed with embedding parameters $m = 9$, $\tau = 6$ and recurrence threshold $\epsilon = 1$. R code to reproduce the figure is available from Xochicale (2018).

5.7 The weaknesses and strengths of RQA

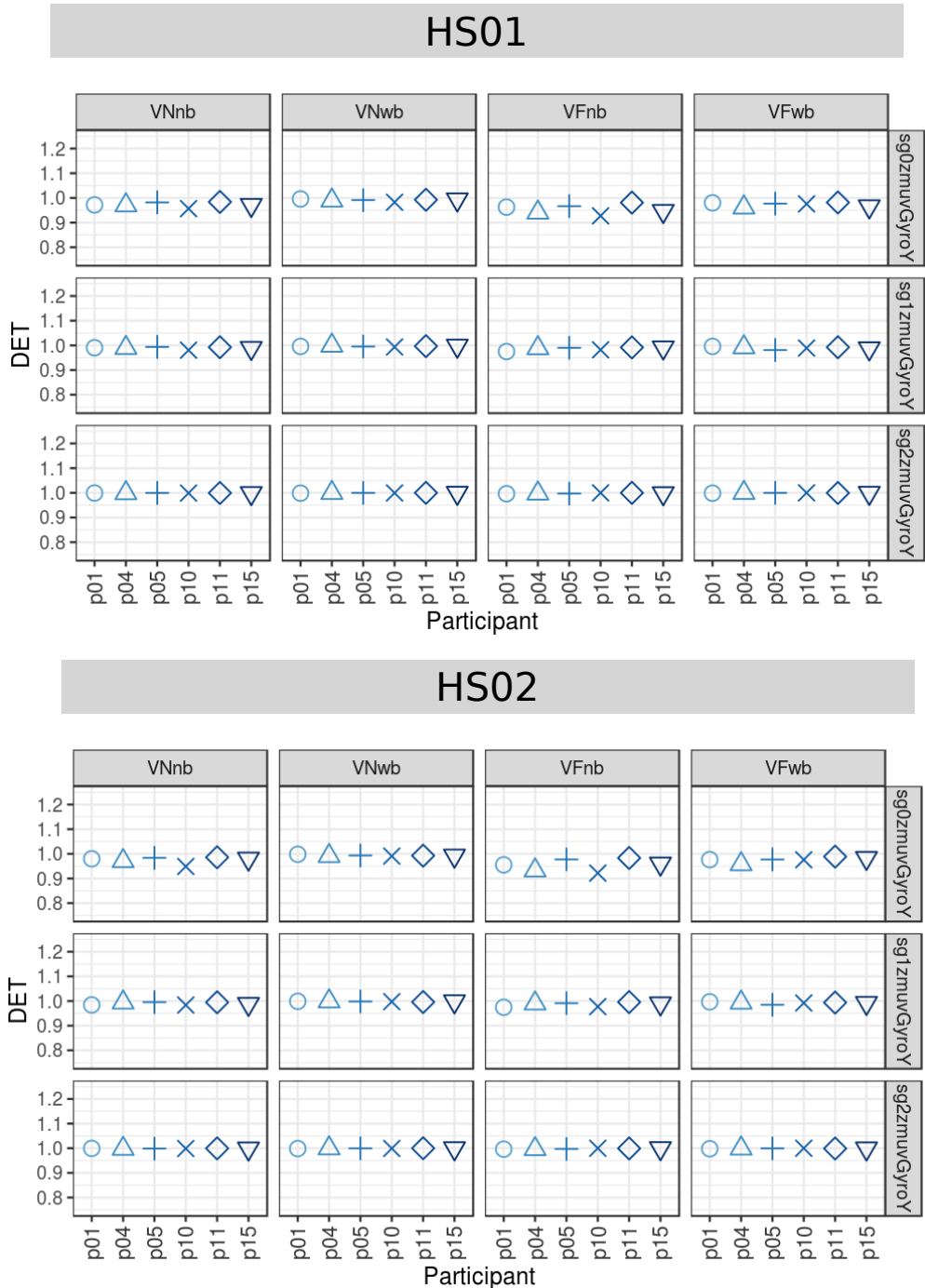


Fig. 5.24 DET values for vertical arm movements. DET values (representing predictability and organisation of the RPs) for 6 participants performing vertical arm movements (VNnb, VNwb, VFnb, VFwb) for sensors HS01, HS02 and three smoothed-normalised axis of GyroY (sg0zmuvGyroY, sg1zmuvGyroY and sg2zmuvGyroY). DET values were computed with embedding parameters $m = 9$, $\tau = 6$ and recurrence threshold $\epsilon = 1$. R code to reproduce the figure is available from Xochicale (2018).

Quantifying Human-Image Imitation Activities

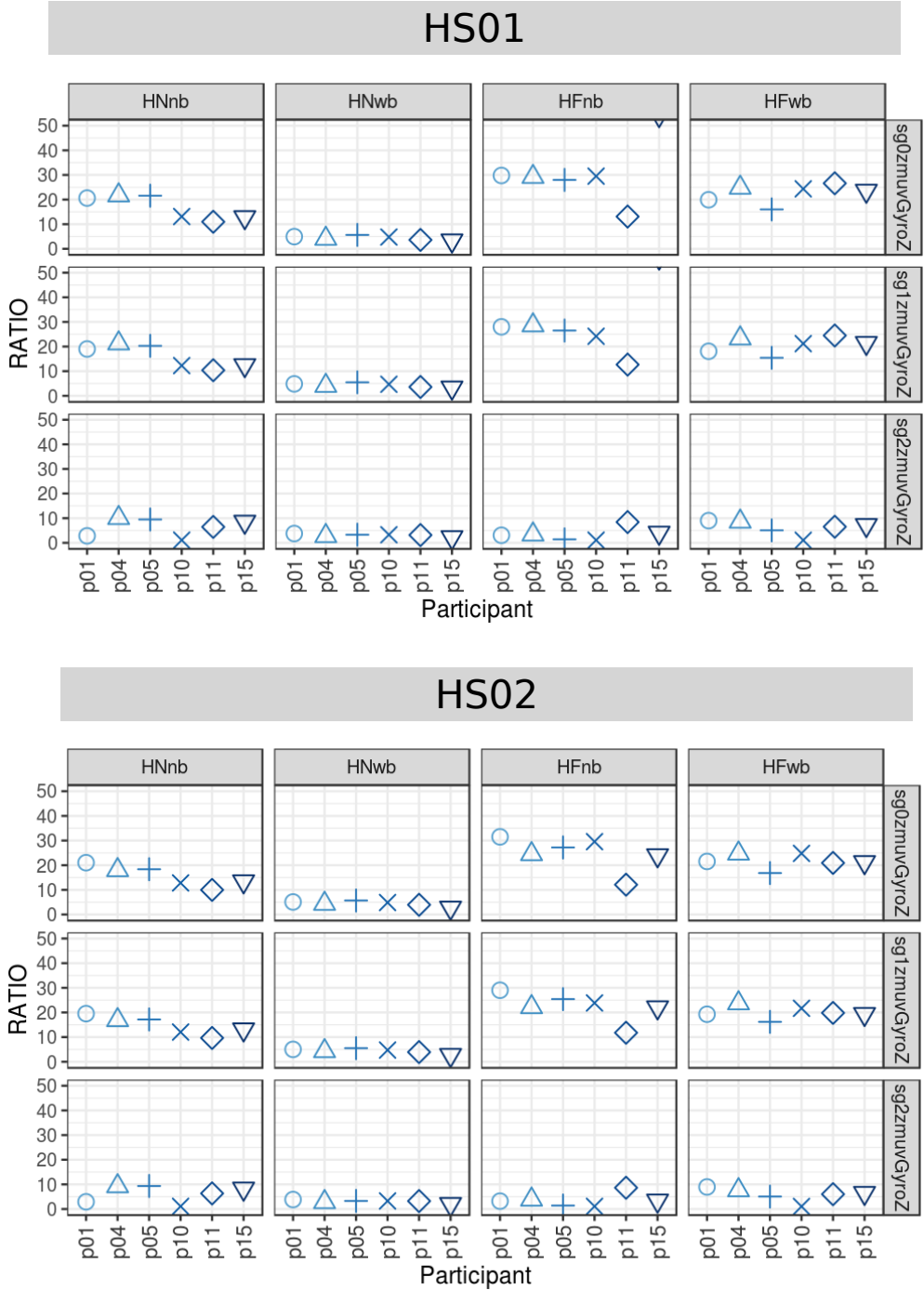


Fig. 5.25 **RATIO values for horizontal arm movements.** RATIO values, representing dynamic transitions, for 6 participants performing horizontal arm movements (HNnb, HNwb, HFnb, HFwb) with sensors HS01, HS02 and three smoothed-normalised axis of GyroZ (sg0zmuvgyroZ, sg1zmuvgyroZ and sg2zmuvgyroZ). RATIO values were computed with embedding parameters $m = 9$, $\tau = 6$ and recurrence threshold $\epsilon = 1$. R code to reproduce the figure is available from Xochicale (2018).

5.7 The weaknesses and strengths of RQA

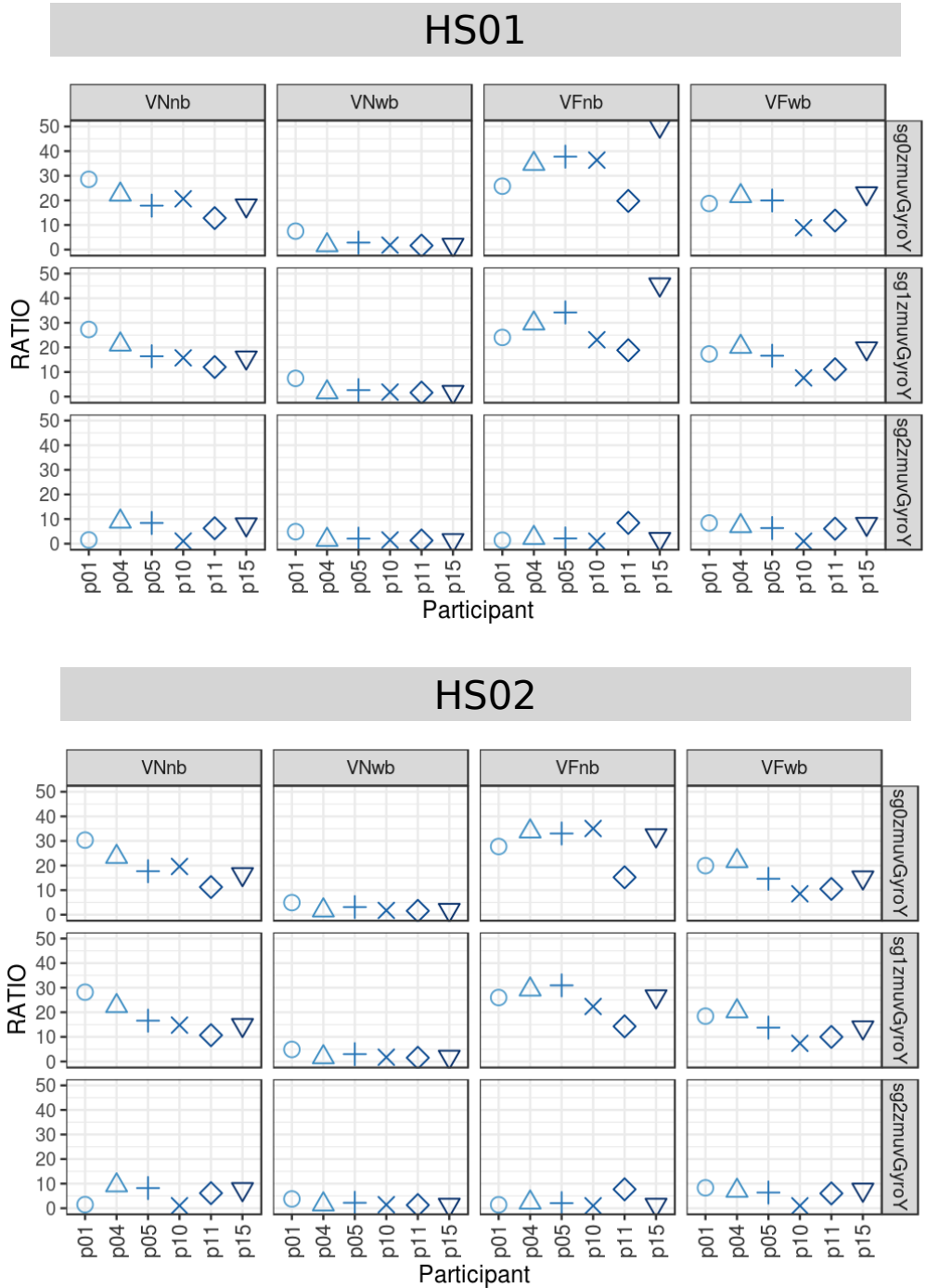


Fig. 5.26 **RATIO** values for vertical arm movements. RATIO values, representing dynamic transitions, for 6 participants performing vertical arm movements (VNnb, VNwb, VFnb, VFwb) with sensors HS01, HS02 and three smoothed-normalised axis of GyroY (sg0zmuvGyroY, sg1zmuvGyroY and sg2zmuvGyroY). RATIO values were computed with embedding parameters $m = 9$, $\tau = 6$ and recurrence threshold $\epsilon = 1$. R code to reproduce the figure is available from Xochicale (2018).

Quantifying Human-Image Imitation Activities

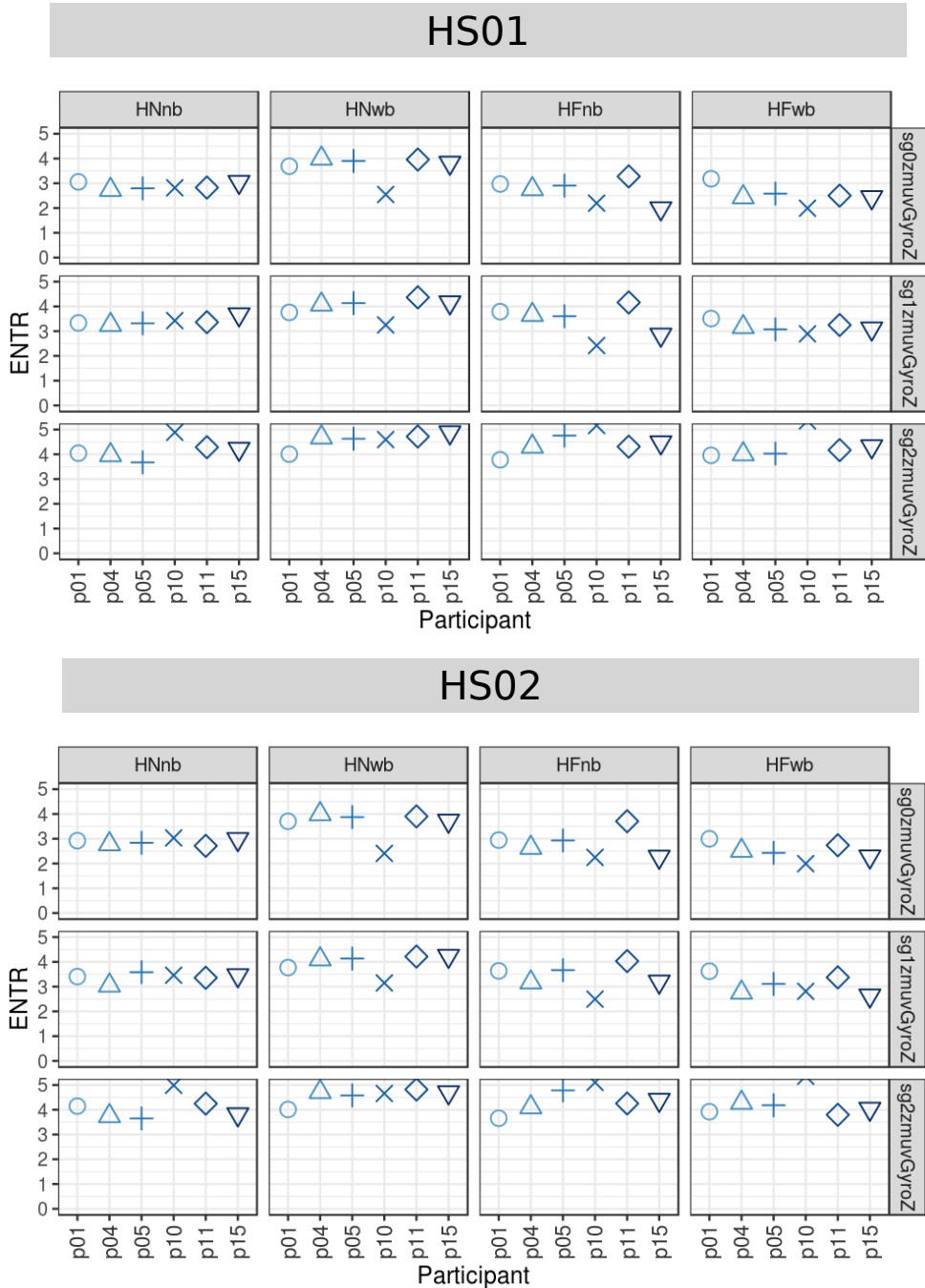


Fig. 5.27 **ENTR values for horizontal arm movements.** ENTR values (representing the complexity of the deterministic structure in time series) for 6 participants performing horizontal arm movements (HNnb, HNwb, HFnb, HFwb) for sensors HS01, HS02 and three smoothed-normalised axis of GyroZ (sg0zmuvGyroZ, sg1zmuvGyroZ and sg2zmuvGyroZ). ENTR values were computed with embedding parameters $m = 9$, $\tau = 6$ and recurrence threshold $\epsilon = 1$. R code to reproduce the figure is available from Xochicale (2018).

5.7 The weaknesses and strengths of RQA

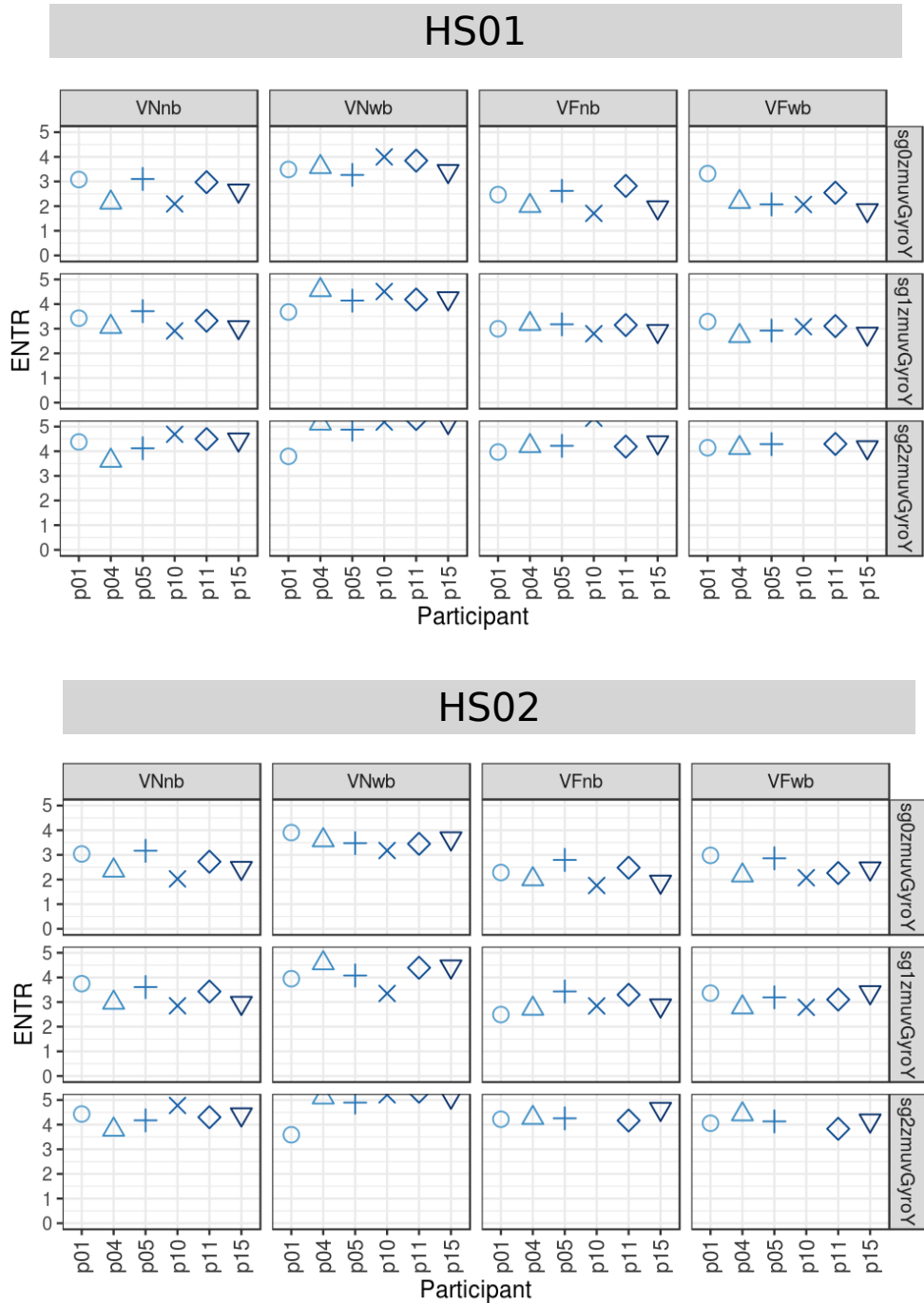


Fig. 5.28 ENTR values for vertical arm movements. ENTR values (representing the complexity of the deterministic structure in time series) for 6 participants performing vertical arm movements (VNnb, VNwb, VFnb, VFwb) for sensors HS01, HS02 and three smoothed-normalised axis of GyroY (sg0zmuvGyroY, sg1zmuvGyroY and sg2zmuvGyroY). ENTR values were computed with embedding parameters $m = 9$, $\tau = 6$ and recurrence threshold $\epsilon = 1$. R code to reproduce the figure is available from Xochicale (2018).

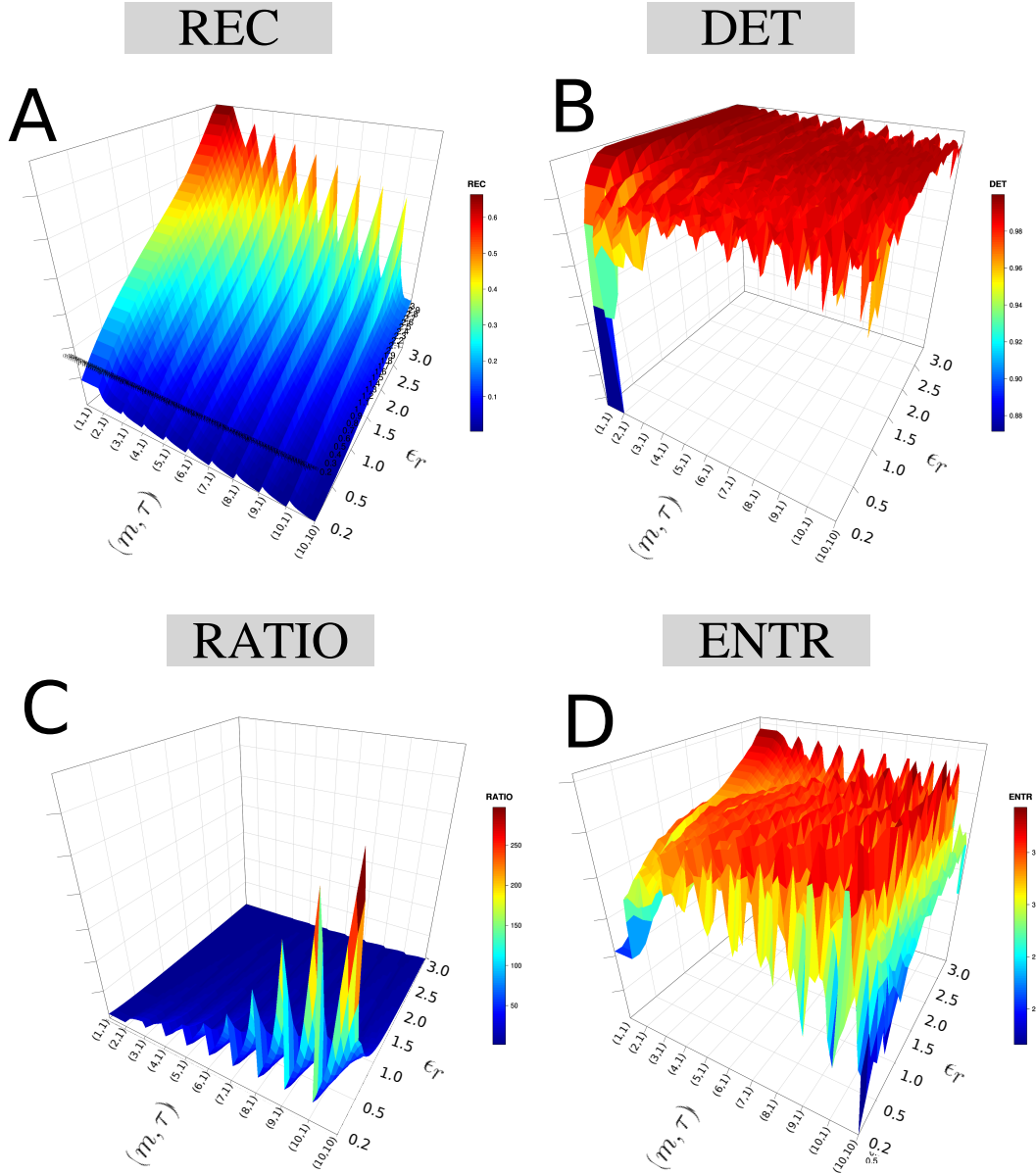


Fig. 5.29 **3D surfaces for RQA metrics.** 3D surfaces for RQA values (A) REC, (B) DET, (C) RATIO and (D) ENTR with an increasing pair of embedding parameters ($0 \leq m \leq 10$, $0 \leq \tau \leq 10$) and recurrence thresholds ($0.2 \geq \epsilon \leq 3$). RQA metrics are computed with the time series of participant *p01* using HS01 sensor, HNb activity, sg0zmuvGyroZ axis and 500 samples for window size length. R code to reproduce the figure is available from Xochicale (2018).

5.7 The weaknesses and strengths of RQA

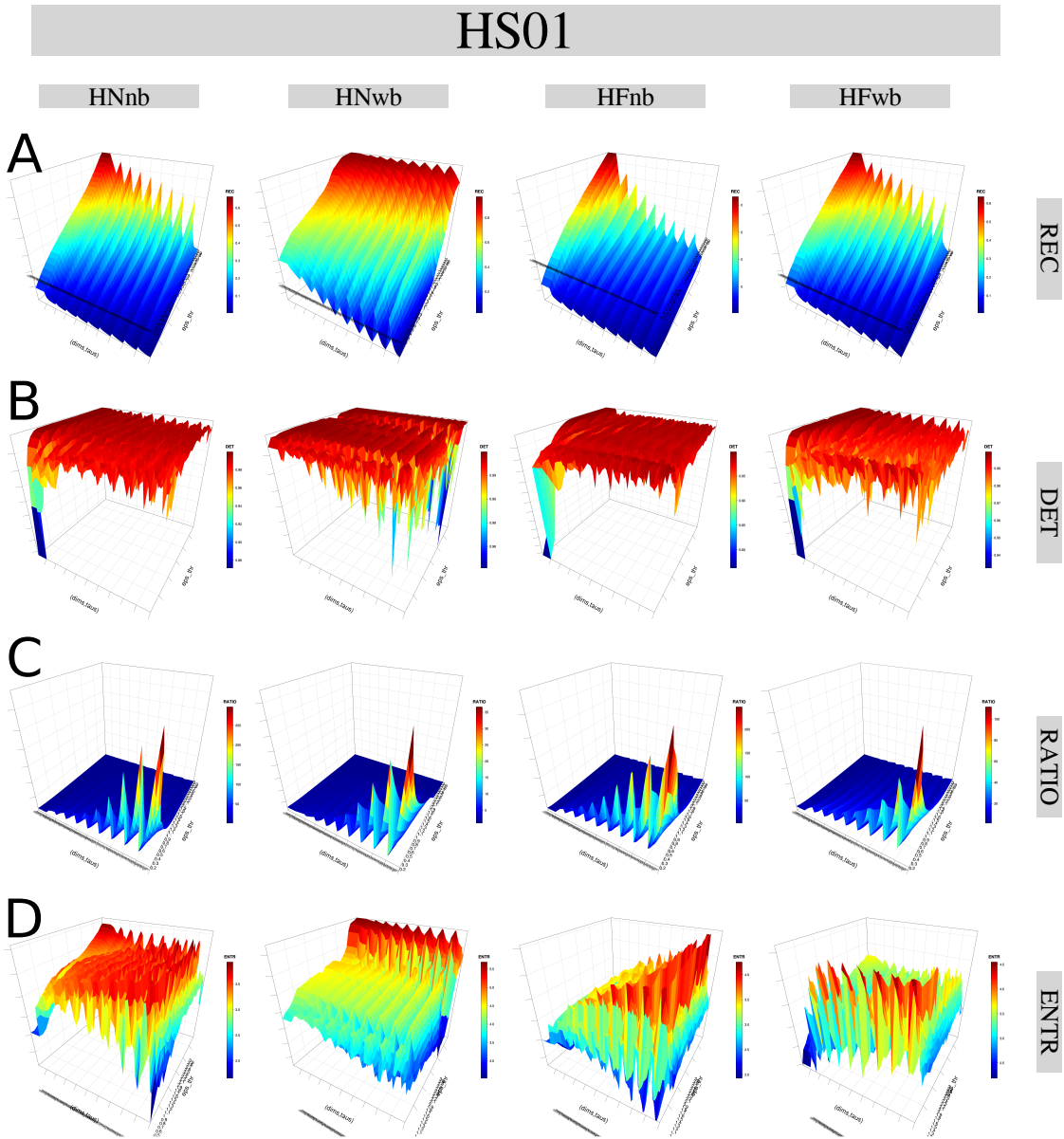


Fig. 5.30 **3D surfaces of RQA metrics for horizontal arm movements with HS01.** 3D surfaces for (A) REC, (B) DET, (C) RATIO and (D) ENTR values with increasing pair of embedding parameters ($0 \leq m \leq 10$, $0 \leq \tau \leq 10$) and recurrence thresholds ($0.2 \geq \epsilon \leq 3$). RQA metrics are computed with the time series of participant p01 for sensors HS01, horizontal arm movement activities (HNnb, HNwb, HFnb, HFwb) and sg0zmuvGyroZ axis with 500 samples window size length. R code to reproduce the figure is available from Xochicale (2018).

Quantifying Human-Image Imitation Activities

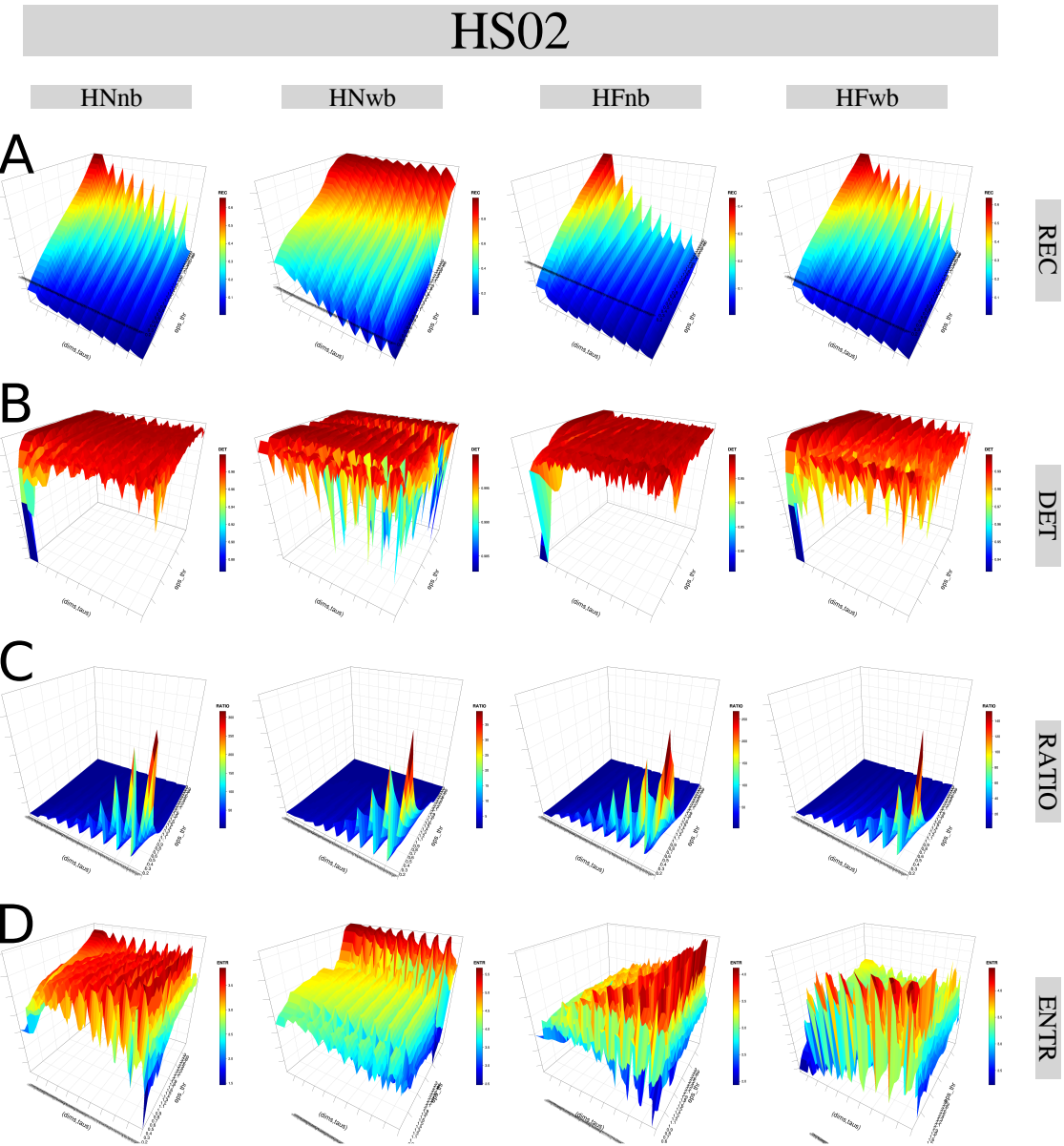


Fig. 5.31 3D surfaces of RQA metrics for horizontal arm movements with HS02. 3D surfaces for (A) REC, (B) DET, (C) RATIO and (D) ENTR values with increasing pair of embedding parameters ($0 \geq m \leq 10$, $0 \geq \tau \leq 10$) and recurrence thresholds ($0.2 \geq \epsilon \leq 3$). RQA metrics are computed with the time series of participant p01 for sensors HS02, horizontal arm movement activities (HNnb, HNwb, HFnb, HFwb) and sg0zmuvGyroZ axis with 500 samples window size length. R code to reproduce the figure is available from Xochicale (2018).

5.7 The weaknesses and strengths of RQA

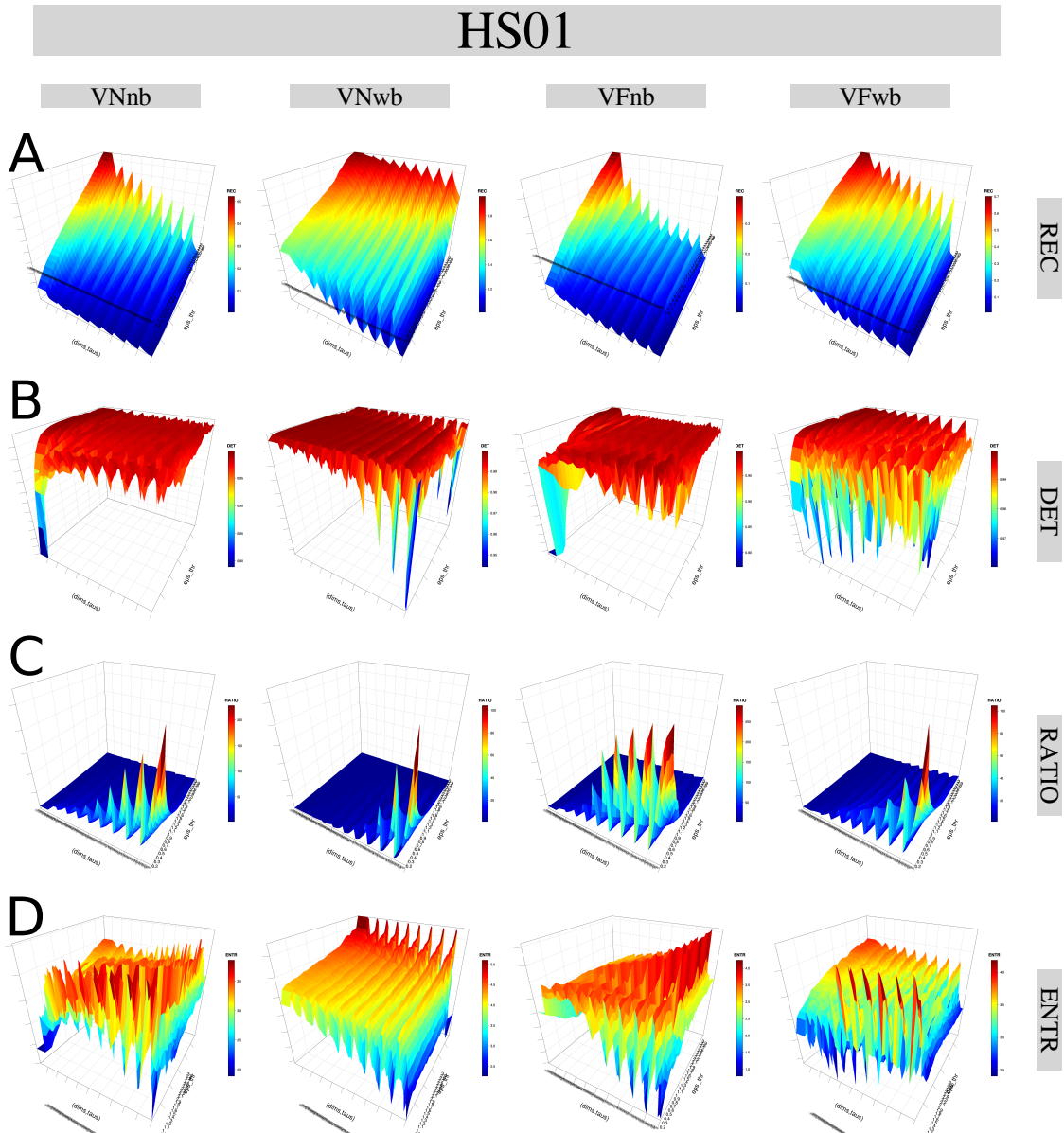


Fig. 5.32 3D surfaces of RQA metrics for vertical arm movements with HS01. 3D surfaces for (A) REC, (B) DET, (C) RATIO and (D) ENTR values with increasing pair of embedding parameters ($0 \geq m \leq 10$, $0 \geq \tau \leq 10$) and recurrence thresholds ($0.2 \geq \epsilon \leq 3$). RQA metrics are computed with the time series of participant *p01* for sensors HS01, vertical arm movements activities (VNnb, VNwb, VFnb, VFwb) and sg0zmuvGyroY axis with 500 samples window size length. R code to reproduce the figure is available from Xochicale (2018).

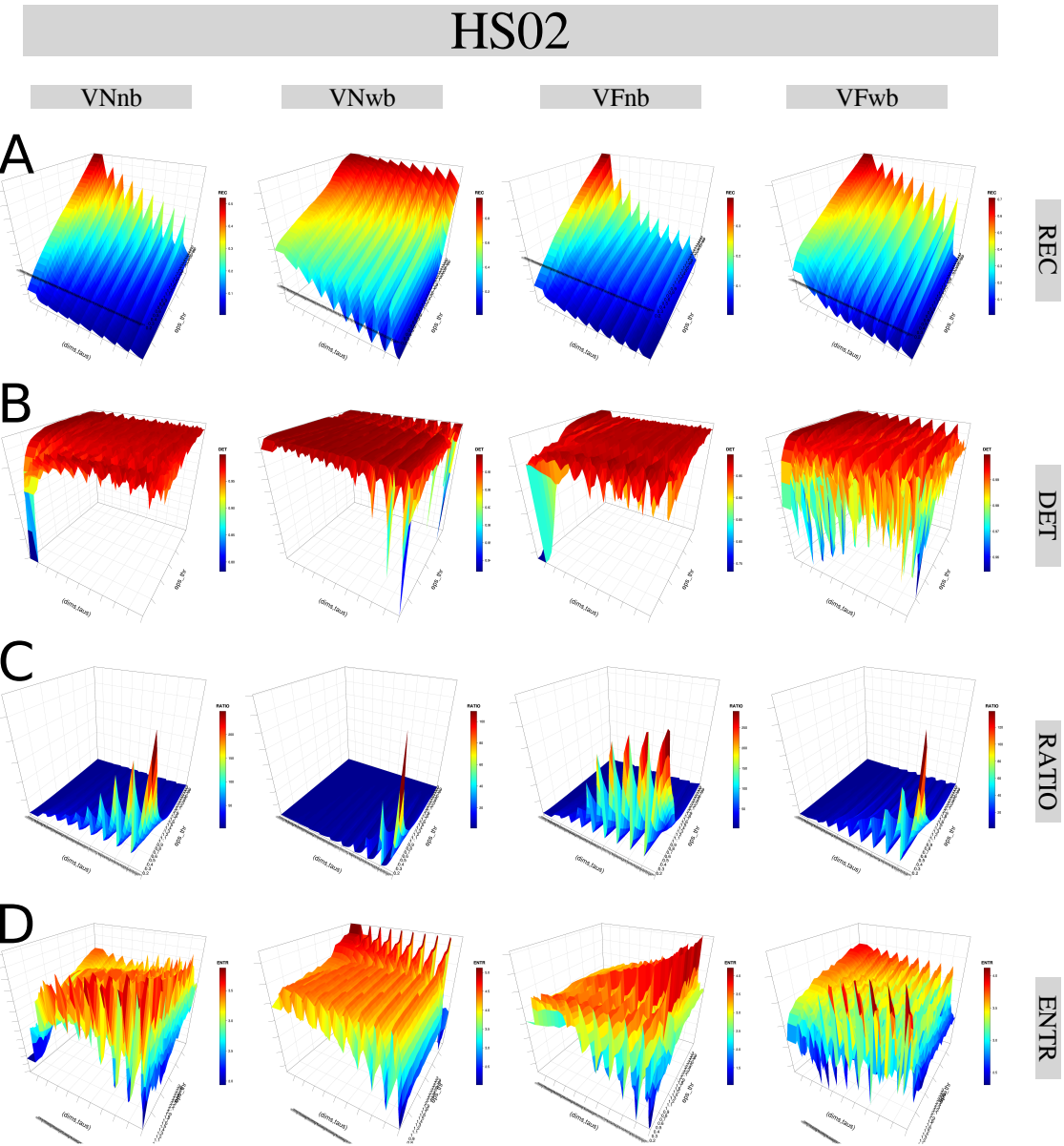


Fig. 5.33 **3D surfaces of RQA metrics for vertical arm movements with HS02.** 3D surfaces for (A) REC, (B) DET, (C) RATIO and (D) ENTR values with increasing pair of embedding parameters ($0 \geq m \leq 10$, $0 \geq \tau \leq 10$) and recurrence thresholds ($0.2 \geq \epsilon \leq 3$). RQA metrics are computed with the time series of participant *p01* for sensors HS02, vertical arm movements activities (VNnb, VNwb, VFnb, VFwb) and sg0zmuvGyroY axis with 500 samples window size length. R code to reproduce the figure is available from Xochicale (2018).

5.7 The weaknesses and strengths of RQA

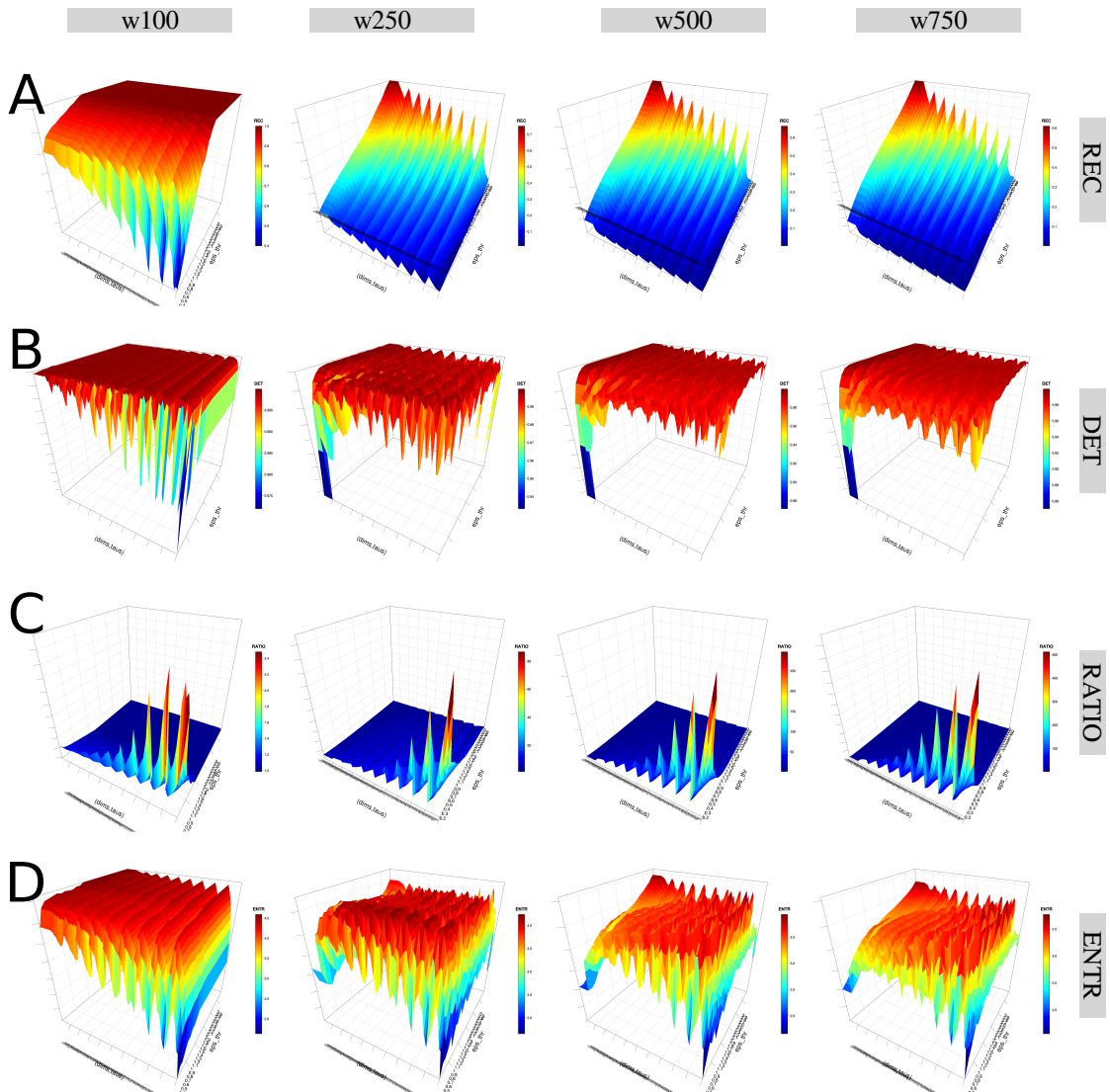


Fig. 5.34 3D surfaces of RQAs metrics for different window size lengths. 3D surfaces of RQA metrics ((A) REC, (B) DET, (C) RATIO, and (D) ENTR) with increasing embedding parameters and recurrence thresholds for four window lengths (w100, w250, w500 and w750). RQA metrics values are for time series of participant p01 using HS01 sensor, HNnb activity and sg0zmuvGyroZ axis. R code to reproduce the figure is available from Xochicale (2018).

Quantifying Human-Image Imitation Activities

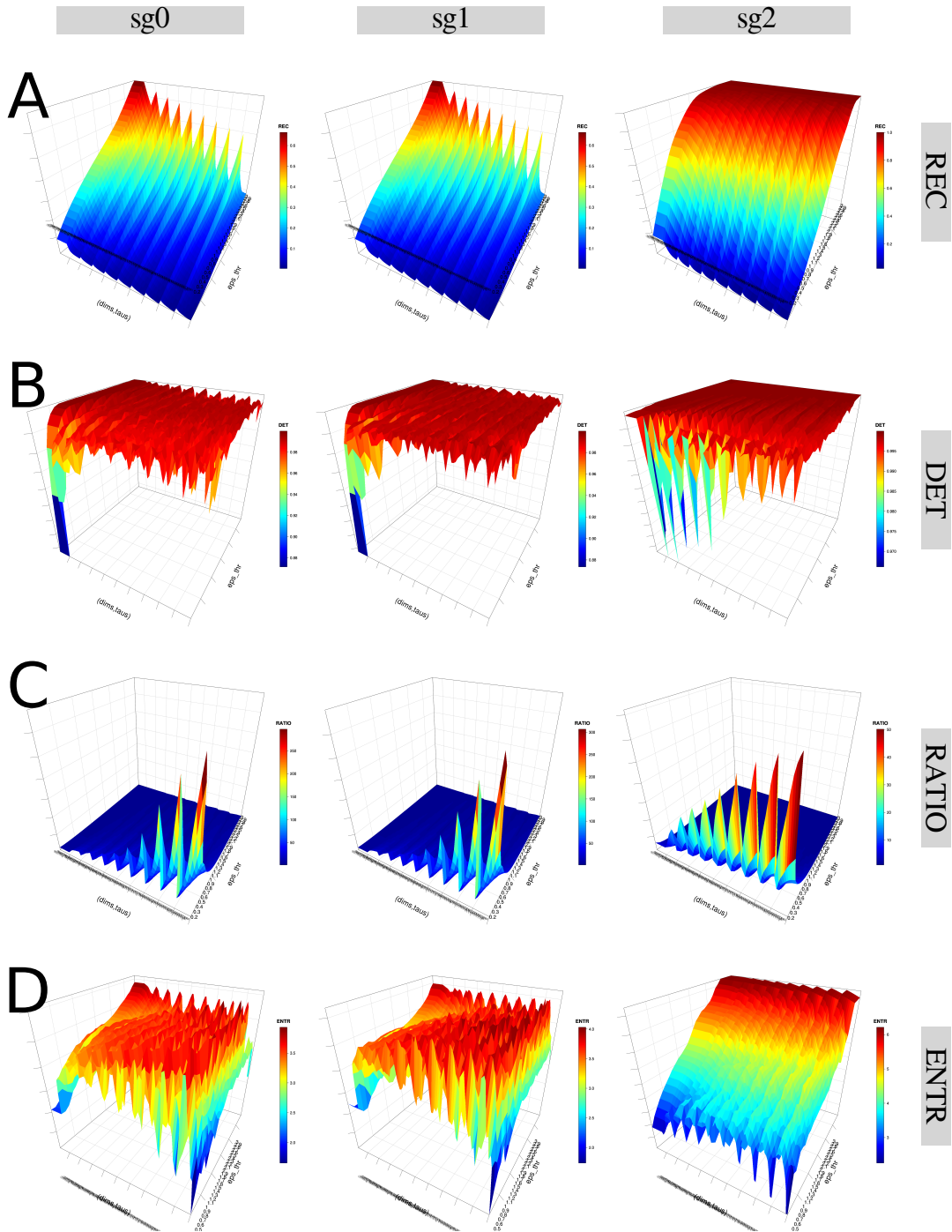


Fig. 5.35 3D surfaces of RQA metrics with three levels of smoothness. 3D surfaces of RQA metrics ((A) REC, (B) DET, (C) RATIO, and (D) ENTR) with increasing embedding parameters and recurrence thresholds for three levels of smoothness (sg0zmuvGyroZ, sg1zmuvGyroZ, and sg2zmuvGyroZ). RQA metrics are computed from time series of participant p01 using HS01 sensor, HNb activity and 500 samples window length. R code to reproduce the figure is available from Xochicale (2018).

5.7 The weaknesses and strengths of RQA

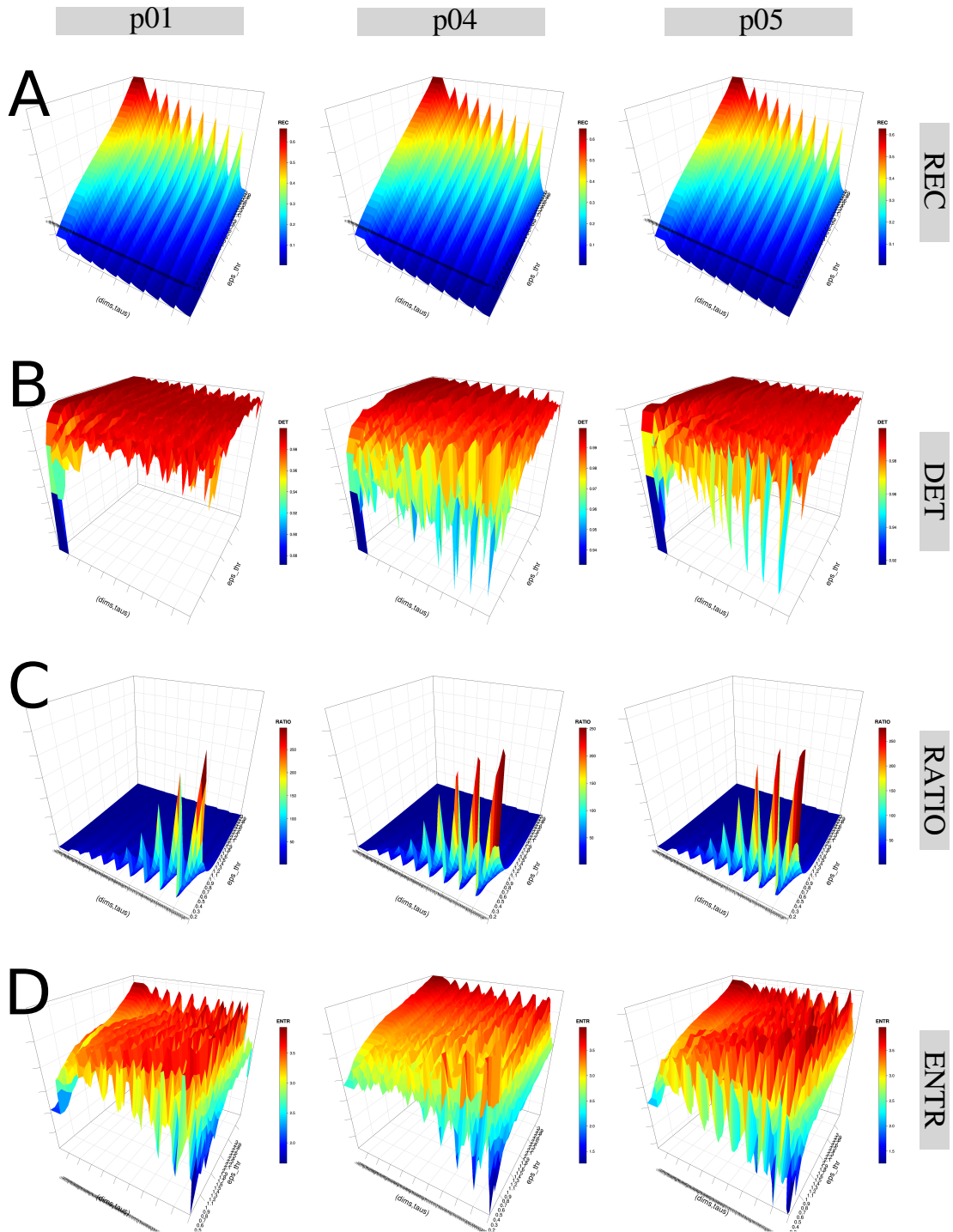


Fig. 5.36 3D surfaces of RQA metrics with three participants. 3D surfaces of RQA metrics ((A) REC, (B) DET, (C) RATIO, and (D) ENTR) for participants *p01*, *p04* and *p05* with increasing embedding parameters and recurrence thresholds. RQA metrics values are for time series of HS01 sensor, HNb activity and 500 samples window length. R code to reproduce the figure is available from Xochicale (2018).

